UNIVERSITAS INDONESIA

CONTRIBUTIONS OF SUB TARGET AND CONFINEMENT EFFECTS IN EXTENSION OF LASER INDUCED SHOCK WAVE PLASMA SPECTROSCOPY TO NON-METALLIC TARGETS

DISERTASI

untuk memperoleh gelar Doktor dalam ilmu Opto-Elektroteknika dan Aplikasi Laser yang dipertahankan di hadapan Sidang Senat Terbuka Senat Akademik Universitas Indonesia di bawah pimpinan Rektor Universitas Indonesia dr. Usman Chatib Warsa, Sp.MK., Ph.D. pada hari Rabu, tanggal 25 September 2002, pukul 10.00 WIB

RINDA HEDWIG

Program Pascasarjana Opto-Elektroteknika dan Aplikasi Laser
Fakultas Teknik
2002

Promotor:

Prof. Tjia May On, Ph.D.
Guru Besar pada Jurusan Fisika
Fakultas Matematika dan Ilmu Pengetahuan Alam
Institut Teknologi Bandung
Guru Besar Luar Biasa pada
Program Pascasarjana Opto-Elektroteknika dan Aplikasi Laser,
Fakultas Teknik, Universitas Indonesia

Ko-Promotor:

Prof. Kiichiro Kagawa, Dr.Eng.Sc.
Department of Physics, Faculty of Education and Regional Studies,
Fukui University, Japan

Ko-Promotor:

Dr. Hendrik Kurniawan
Program Pascasarjana Opto-Elektroteknika dan Aplikasi Laser,
Fakultas Teknik, Universitas Indonesia

Panitia Penguji:

1. **Prof. Muhammad Barmawi, Ph.D.**
2. **Prof. Dr. Rustam Effendi Siregar**
3. **Prof. Dr. Andrianto Handojo**
4. **Prof. Dr. Sardy S.**
5. **Dr. Muhammad Hikam**

ABSTRACT

An comprehensive study has been carried out for the study and extension of laser induced shock wave plasma spectroscopy (LISPS) application to non metallic soft and hard samples. For this purpose, a series of experiments were conducted to investigate the dynamical process taking place in the laser plasma generated by a high power and short pulse laser irradiations on a non metal soft and hard samples. It was found that in the case of non metal soft sample, the ablated atoms failed to induce a visible plasma at the surface of the target due to the gushing speed of the atom is very low. With the support of a sub target however, it became possible, after a few laser shots depending on the target layer thickness, to generate the shock wave plasma emitting the characteristic spectral lines of the target material.

Another related phenomenon studied in this experiment is the pre-irradiation effect observed on a non metal hard sample such as quartz sample, which was characterized by the absence of secondary plasma at the initial shots. The disappearance of this effect at a later stage was found to be connected with the appearance of a crater of appropriate depth on the sample surface created by initial repeated irradiations on the sample surface. The plasma produced thereafter exhibited typical features of a secondary plasma. Further experiment employing artificial ring crater on the sample surface has eliminated the pre-irradiation effect completely, and has thus demonstrated that it is the confinement effect of the crater which was solely responsible for the generation of secondary plasma from the non metal hard target. This conclusion is in conformation with the shock wave model proposed earlier.

These experimental studies have thus considerably substantiated our understanding of the process of secondary plasma generation. In turn, this result helps to improve the quality and extend the scope of LISPS applications in the future.

Keywords:

laser-induced shock wave plasma, soft sample, sub target effect, spectrochemical analysis, confinement effect

ACKNOWLEDGEMENT

spectroscopy. It was the knowledge I gained from these resources that made this thesis possible.

- The same thankful also goes to all my colleagues in Bina Nusantara University, especially those who work in Hardware Laboratory. Their cooperative works did support some of my tasks that I had no chance to finish.
- Last but not least, I apologize to all those who helped that I did not acknowledge specifically. I believe there were many appreciate your assistance.

LIST OF CONTENTS

LIST OF FIGURES

LIST OF TABLES

LIST OF ABBREVIATIONS

LAESA   : Laser Ablation Emission Spectrochemical Analysis

LISPS   : Laser Induced Shock Wave Spectroscopy

LIBS   : Laser Induced Breakdown Spectroscopy

AAS   : Atomic Absorption Spectrometry

AFS   : Atomic Fluorescence Spectrometry

ICP   : Inductively Coupled Plasma

TEA   : Transversely Excited Atmospheric

FWHM   : Full Width Half Maximum

OMA   : Optical Multichannel Analyzer

EPMA   : Electron Probe Micro Analysis

UV   : Ultra Violet

Nd-YAG   : Neodymium Yttrium Aluminum Garnet

Chapter One

GENERAL INTRODUCTION

Spectrochemical methods of analysis are among the most widely used analytical methods. The application of spectrochemical methods ranges from qualitative analysis to the determination of quantitative composition of materials as well as detection of trace elements of great importance. As a result, they have been widely used for process control and product quality assessment as well as environmental monitoring. The most popular among the existing technique are Atomic Absorption Spectrometry (AAS), Atomic Fluorescence Spectrometry (AFS), and Atomic Emission Spectrometry. Each method has its advantages and disadvantages. For instance, AAS method which has become the most widely used single-element technique for the determination of metals, operates on the basis of absorption spectra from the neutral, ground-state atoms produced by an atomizer.[1] AAS has been used to determine metals and some nonmetals in almost every conceivable type of samples. Many standard procedures for water analysis are based on AAS, except for water samples with a high salt content; the analysis is usually straightforward. The use of AAS in the metallurgical and mining industries is common for analysis of metals, alloys, geochemical samples and electroplating solutions. However, this method requires tedious sample preparation procedure. Analysis of petroleum products for example, presents special sample preparation difficulties. For biological and clinical samples, it is critical to remove the organic matrix by digestion or some other method before analysis.

The AFS method which is a sensitive and powerful technique for detecting molecules and atoms, boasts the often cited advantages of low detection limit, large linear dynamic ranges, multi-element capabilities, simplicity, and freedom from spectral interferences. Its overall detection limit are not generally better and often worse than those reported for AAS except for few elements. In terms of dynamic range and multi-element capability, atomic fluorescence spectrometry is superior to AAS, but comparable to AES. Nondispersive AFS systems based on conventional excitation sources can be relatively simple and inexpensive.[1]

The AES method has great potential as a qualitative and quantitative tool since all elements can be made to emit characteristic spectra under the appropriate conditions.

Lockyer stated in 1874 that *while the qualitative spectrum analysis depends on the position of the lines, the quantitative analysis depends on their length, brightness, thickness and number.*[2] The spark discharges were first used to obtain spectra from solution and various spark sources were developed with static electrical sources. It has now become common to use high-voltage, low-current oscillatory discharge with voltages of 10,000–50,000 V. The arc gave very intense and therefore sensitive spectra, but the reproducibility was poor. The electronic temperature was in the order of 6000–8000 K, and under these conditions metal electrodes melted and vaporized directly. This was an advantage because many metals and alloys can be analyzed directly, avoiding any pretreatment which may introduce errors. The advantage of using AES is mainly its direct applicability to elemental detection using simple equipment compared to any other method.

In the mean time, the advent of lasers has greatly expanded the field of spectroscopy in many areas since tunable lasers have now been obtained at wavelengths covering the range from far-infrared to ultra-violet region. The use of laser sources are making it possible to obtain information that was difficult or impossible to obtain with conventional sources.[3]

The method of laser atomic emission spectrochemical analysis (LAESA) was first introduced by Brech[4] in 1962. Its potential as a sensitive and convenient tool for microanalysis was henceforth quickly recognized. Thanks to the continued improvement in its detection sensitivity and sample applicability in addition to the advantage of rapid analysis without the need of sample pretreatment, this method has gained growing acceptance in wide ranging field of spectrochemical applications. This technique has many advantages compared to other analytical methods which exhibits several attractive features such as the ablated matter is sufficiently atomized to permit analysis by auxiliary methods requiring material in the atomic state, thus eliminating the time-consuming steps which involved in sample preparation. Moreover, the laser pulse can ablate material for in situ analysis and microanalysis can be obtained due to the small size of the laser spot at its focal. Also, laser ablation minimize the amount of sample used in the analysis[3] and reduced surface damaged caused by laser bombardment.

Nevertheless the more conventional LAESA method suffers from some drawbacks, in particular the intrinsically large background which can only be partially overcome by the use of expensive detecting system. This background of emission is

very strong due to high density and high temperature plasma which made the S/B ratio relatively low, and detection limit becomes low sensitivity. Besides, self-absorption of the emission line takes place to a remarkable extent due to the generation of large temperature difference between the inside and outside of the plasma, which brings about the non-linear calibration curve.[3] In addition to this, in LAESA method some problems were also observed when analysis is done for non metal soft sample or applied to non metal hard sample.

In a later development, an alternative method was initiated in the studies of plasma emission induced by a high power and short pulse laser on a target surrounded by air at reduced pressures.[5-12] It was found that the laser plasma produced invariably consists of two distinct parts. The first part occupies a small region of high temperature (the primary plasma), which gives rise to an intense and continuous emission for a short time, right above the surface of the target. The second part (the secondary plasma) expands with time around the primary plasma, emitting sharp atomic spectral lines. These characteristics of the secondary plasma has led to its special advantages for highly sensitive spectrochemical analysis. Among these favorable characteristics are, the low background emission spectrum; the good linearity between the emission intensity and the content of the element most remarkable. The symmetrical hemispherical shape which leads to high precision analysis and high excitation temperature brings to high sensitive analysis are also advantages.

By means of time-resolved measurements in our experiments using a TEA CO_2 laser[7] and an excimer laser,[6] we were able to demonstrate that this secondary plasma was induced by a shock wave generated in the surrounding gas, while the primary plasma acted as a source of explosion energy. It was further shown that the atomic emission in the plasma was also the result of thermal excitation made possible by the shock wave which proved by density jump experiment.[13] We refer to this method as laser-induced shock wave plasma spectroscopy (LISPS). There are two obvious practical applications of LISPS; one is its application to the rapid inspection of industrial products, such as steel[6] and glass samples,[8] and the other is the application to the field-based spectrochemical analysis of mining or geological samples.

It has been recognized generally that the characteristics of a laser plasma depend on a number of factors involved in the process. Three of these factors are assumed to be most important. One is the surrounding gas conditions such as the kind of gas and

its pressure. Another is the characteristics of the laser light itself such as the wavelength, pulse energy, pulse width and the power density. In addition to this, it also has been noticed in the case of LISPS, that hardness of the target also influences considerably the plasma characteristics. In fact, the generation of all secondary plasmas reported previously were observed on solid metallic targets.[6,7] In order to examine the applicability of LISPS to non metallic samples, the possibility of generating secondary plasmas from such targets must be investigated.

In this study, two types of non metallic targets are used. One consists of non-metallic soft targets, and the other consists of non metallic hard target. In addition to the purpose of extending the application of LISPS to non-metallic samples, these experimental works are also aimed at examining the validity of the laser induced shock wave model which has been established for secondary plasma generated from metallic targets. It will be shown that in the case of unsupported soft target, the secondary plasma simply fails to show up, while the use of target immediately restores the condition for normal formation of the secondary plasma. In the case of hard target, the formation of secondary plasma is preceded by a pre-irradiation effect in the few initial laser shots, which may lead to intolerable damage to the sample surface in some specific applications. It will be shown in this study that this problem too can be properly overcome by the use of artificial crater.

Chapter Two

ROLE OF LASERS IN SPECTROCHEMICAL ANALYSIS

2.1. Spectrochemical Applications of Laser Ablation Technique

When a high irradiance (of the order of GW cm^{-2}) laser beam reaches a solid target, an explosion occurs and a plasma is formed (laser spark). The mechanism of interaction has been well studied but remains less than completely clear. The name 'laser ablation' is generally used, and preferred to laser explosion, although the term 'laser-material interaction' would seem more appropriate since it does not imply a mechanism.[14] The plasma formed can be investigated by monitoring, in a time resolved manner by its spectral emission behavior or by evaluating several of its parameters, at variable delay times, with another laser tuned at a given atomic transition energy and measuring the resulting absorption, fluorescence or ionization signal. On the other hand, the material removed from the target can be transported into practically every other analytical source (flames, graphite furnaces, glow discharge and especially ICPs) for subsequent absorption, emission or ionization measurements. In the later case, the laser is only used for sampling. Laser sampling has the obvious important advantage that it offers direct sampling from any material and without sample preparation. The physical mechanisms and associated methods of technical implementation for spectrochemical applications are listed and described in table 2-1.

The analytical use of the plasma formed by high intensity laser bombardment on a target has been well known since the early 1960s.[15] There are several reasons why the interest in this well known laser method has been revived and is currently enjoying so much success. We can see the number of acronyms used for it, collected in table 2-2, as well as the variety of target materials and applications collected in table 2-3. The increasing need to incorporate more on-line control devices in industrial processes has undoubtedly acted as trigger, but probably the major reasons have to be found in the technological development of good, intensified CCD detectors together with the capability of handling a large amount data, and the availability of compact, cheap and reliable Nd:YAG lasers. The simultaneous multi-element potential, coupled with the rapidity of analysis, is retained here and the sensitivity is

adequate for many applications as indicated at table 2-3. When the technique is used for quantitative microanalysis, matrix effects are considered to be the major drawback, although normalizing parameters such as vaporized mass and the plasma excitation temperature allows for an efficient correction of such effects.

Table 2-1 A sample of commonly used techniques.

Absorption	Use lasers as primary sources for atomic and molecular absorption measurements. Absorbing species are generally located outside the laser cavity, but can also be present inside (intracavity absorption)
Emission	Use lasers tightly focused on a solid, liquid or gaseous sample to create plasma from which atomic and ionic emission of the target constituents is measured
Fluorescence	Use lasers as excitation sources to pump atoms into selected excited states from which radiative de-excitation is measured. Atoms are generated independently outside the laser cavity, but can also be present inside (intracavity fluorescence)
Ionization	Use lasers to pump atoms in highly excited levels from which collisional ionization occurs or to photoionize selectively the atoms (resonance ionization). The charges produced are introduced into a time-of-flight mass spectrometry
Ablation	Use lasers as a sampling device to generate atoms, molecules and particles from a target sample, which are transported into an excitation source, e.g., a plasma

Table 2-2. Laser induced plasmas: semantical variations on the theme.

LAAS	Laser spark spectroscopy
LIBS	Laser induced breakdown spectroscopy
TRELIBS	Time resolved LIBS
FOLIBS	Fiber optics LIBS
LIESA	Laser induced emission spectral analysis
LAESA	Laser ablation emission spectrochemical analysis
LIPS	Laser induced plasma spectroscopy
LISPS	Laser induced shock wave plasma spectroscopy
LA-OES	Laser ablation-optical emission spectroscopy
LALM	Laser ablation in a liquid medium
RSP	Repetitive spark pair

Some of these techniques are characterized by extremely high detection sensitivity for selected elements, while others can be used for real time, simultaneous monitoring of

many elements in different samples of environmental interest. Referring to the ionization technique, for instance, it has been repeatedly stressed theoretically and demonstrated experimentally that it possesses several unique characteristics such as single atom or single molecule detection limit, spectral resolution limited only by the homogeneous linewidth, temporal resolution below picosecond, spatial resolution of the order of the De Broglie wavelength of the electron or ion, selectivity which can reach 1 X 10^{20} and finally applicability to any atom or molecule. Single ion absorption and fluorescence are also possible from the theoretical point of view.

Table 2-3. Target materials and selected applications of laser induced plasma spectroscopy.

Electronic substrates
Nuclear materials
Glasses – ceramics
Polymer materials
Marble cleaning – art conservation
Chemical imaging – element mapping
Microanalysis of alloys – depth profiling
Particulate in combustion environments
Trace pollutants in soil, sand, sewage
Metal aerosol emission
Particle detection and counting
Atomization of solid targets in a liquid medium

Despite these impressive characteristics, it is known that the large majority of laser systems used are complex to operate and expensive to acquire. The many statements made, both in the literature and in specific round table discussions held at scientific meetings, that the use of lasers in routine analytical applications will always be limited to few selected applications were more or less justified. Consequently, it appeared that laser methods could be eliminated as viable contenders for near-term routine atomic spectrometric measurements.[15] However, this picture has changed dramatically thanks to a series of remarkable advances achieved in the near future due to commercial development of tunable solid-state laser, as well as other developments which will be described in the latest part of this chapter.

In the following sections, we will start our discussion on laser ablation emission spectrochemical analysis (LAESA), and proceed with more recent developments in the field including especially the one applied at low pressure surrounding gas, where during its application we found phenomenon which will be clarified in this thesis.

2.2. Laser Ablation Emission Spectrochemical Analysis (LAESA)

LAESA is a typical application for high power pulse lasers. This technique has many latent advantages over other analytical methods which exhibits several attractive features, especially compared to ordinary AES method. First, in many cases, the ablated matter is sufficiently atomized to permit analysis by auxiliary methods requiring material in the atomic state, thus eliminating the time-consuming steps sometimes involved in sample preparation. Second, the laser pulse can ablate material for analysis at a remote location. Third, all types of material can be sampled with the laser spark because ablation is accomplished by focused light energy and does not rely on the electrical properties of the material, as does ablation via conventional electrode sparks. Fourth, the small spot size of a focused laser pulse can provide a spatially resolved microanalysis of a surface. Fifth, laser ablation minimize the amount of sample used in the analysis. The last, many of the auxiliary techniques have greater detection sensitivities, dynamic ranges, and freedom from matrix effects than direct spectroscopic analysis of the laser plasma. Combining these techniques with laser ablation permits use of these improved capacities together with the rapid sampling provided by the laser spark.[16] On the other hand, the disadvantages of this method is that the background of this emission spectrum is very strong due to high density and high temperature plasma, self-absorption of the emission line takes place to a remarkable extent due to the generation of large temperature difference between the inside and outside of the plasma, which brings about the non-linear calibration curve.[17] As the result, the LAESA method was mainly used only for qualitative analysis or semi-quantitative analysis, and the research of LAESA had become inactive since in the early of 1980s.

Nowadays good quality laser system such as YAG is commercially available offering good shot to shot power stability and good beam quality which brings high focusibility of the laser light. Also the development of optical multi-channel analyzer (OMA) has contributed to the study of laser spectroscopy. Supported by these new instruments, recently the study of LAESA has become revival because the LAESA is still attractive to spectrochemist as the rapid quantitative analytical method for solid samples.

Roughly speaking, nowadays there are two main streams of development in this study. The first adopts a high-pressure surrounding gas, which has been developed by

Radziemski and Cremer's group and is usually called laser-induced breakdown spectroscopy (LIBS).[2,18] In this method high peak power with short duration laser such as Nd:YAG laser was focused onto the sample at atmospheric pressure. In order to remove the disturbing background spectrum coming from high temperature and high density plasma, gated OMA was effectively incorporated in the detection system. Another stream of development in LAESA is the use of low gas pressure and we refer to this method as laser-induced shock-wave plasma spectroscopy (LISPS).[5-11]

2.3. Laser-Induced Shock -Wave Plasma Spectroscopy (LISPS)

LAESA for low pressure surrounding gas[17] is observed when laser plasma is produced under reduced pressure aiming the deduction of the background emission intensity in the spectrum. We have shown in our previous experiments that laser-induced shock wave plasma is generated when a pulse laser such as N_2 laser, TEA CO_2 laser, or excimer laser and YAG laser, is focused onto a solid target at a reduced gas pressure of around 1 Torr.[5-8] The laser plasma consists of two distinct region. The first is a small area of high temperature plasma (the primary plasma), which gives off an intense, continuous emission spectrum for a short time just above the surface of the target. The second area (the secondary plasma) expands with time around the primary plasma, emitting sharp atomic spectral line spectrum with negligibly low background signals. Atoms in the secondary plasma are excited by the shock wave, while the primary plasma acts as an initial explosion energy source. We have referred this method as laser-induced shock wave plasma spectroscopy (LISPS).

We have also proved that the laser-induced shock wave plasma is excellent light source for emission spectrochemical analysis. In ordinary atomic emission spectrometry, such as arc discharge method and spark discharge method, atoms are excited by means of an electric discharge. In general, in atomic emission spectrometry the detection limit of the elements is mainly determined by the intensity of the background emission, which arises from the process of electron-ion recombination or the electron-ion bremsstrahlung.[19] The lower the background emission intensity, the lower the minimum determinable concentration of the elements. In contrast to this, in plasma induced by the shock wave at low pressures, the background emission intensity is expected to be considerably reduced, because in the shock wave plasma the excitation of the atoms takes place by means of a purely thermal process, without

employing any electric fields, and the excitation process is substantially a non-equilibrium process.

This secondary plasma has characteristics quite favorable to spectrochemical analysis. Among these positive characteristics are, low background emission spectrum and good linearity between the emission intensity and the content of the element are representative. The symmetrical hemispherical shape which leads to high precision analysis and high excitation temperature brings to high sensitive analysis are also advantages. There are two obvious practical applications of LISPS; one is its application to the rapid inspection of industrial products, such as steel and glass samples, and the other is the application to the field-based spectrochemical analysis of mining or geological samples.

It can be said that this LISPS method has substantially high prospect to compete with ICP spectrometry when we use this LISPS method for inspection of homogeneous samples of industrial products. In order to prove this practical quantitative experiment should be made using polychromator in the near future.

At present EPMA (Electron Probe Micro Analysis) is widely used to make micro analysis on the small minerals in rock samples. However, for this purpose the sample surface must be polished flatly with high precision, and therefore it takes time for pretreatment. In contrast to this in our method, rapid quantitative analysis can be made with more high sensitivity because in our method required flatness is not so sever and the required pressure condition can be easily obtained using air. Also in our method compact requirement can be realized by combining small pulse laser with a pulse energy of several mJ and OMA for spectrum detection system. Such compact equipment can be easily moved by a car and quantitative analysis can be made in outdoor. It is expected that our LISPS method will be used effectively in the field of mining industry and geological science.

2.4. The Limitation of LISPS Method

Despite the remarkable progress described in the preceding action, demonstrating viability of the LISPS technique for various high sensitivity spectrochemical detection, this method remains restricted to metallic and certain hard targets (such as ruby, ceramic and other hard oxide materials). In the case of light oxide materials (such as glass and agate), this technique suffers from pre-irradiation effect, and

becomes inapplicable to even softer target such as silicone grease. These problems are expected to have their origin in the effectiveness in the generation of shock wave required for the formation of the secondary plasma.

This research is aimed at overcoming those limitation mentioned above. To this end the condition of shock wave generation will be reexamined. A series of experiments are performed for this study, and special techniques are devised to get around the problems stated above in order to extend the applicability of the LISPS technique. These experiments and the results obtained as well as the techniques developed will described respectively in the following sections.

SUB TARGET EFFECT ON TEA CO$_2$ LASER INDUCED PLASMA FROM SOFT SAMPLE

3.1. The Role of a Sub Target in Laser Plasma Generated at Low Pressure

3.1.1 Introduction

The characteristics of a laser plasma depend on some factors involved in the process. Three kinds of factors are assumed to be most important. One is surrounding gas conditions, another is the characteristics of the laser light itself and in addition to this, in the case of LISPS, hardness of the target also influences the plasma generation. In fact in LISPS using TEA CO$_2$ laser, some problems were observed in the case of a soft material, such as low melting point glass[8] or biological samples, where shock wave plasma could not be generated. We understood this phenomenon by assuming that the soft target absorbs recoil energy and atoms gushing from the primary plasma do not acquire sufficient speed to form a shock wave. If the process is true, we can overcome this problem by setting the sub target on the back of the sample so as to produce the repulsion force by which the gushing speed of the atoms is increased. In order to prove this, the present study was undertaken using mainly silicon grease as a sample.

3.1.2. Plasma Generation at Low Pressure Surrounding Air

A TEA CO$_2$ laser (Lumonics, multigas laser, model HE-440B, set at 100 mJ, FWHM 100 ns) was used in the present experiments. The actual pulse energy, however, which was focused on the target was roughly 50 mJ. During this experiment the laser was operated shot by shot, and the power fluctuations were determined to be less than 5%.

The laser radiation was focused by a ZnSe lens (f = 100 mm) through a ZnSe window onto the surface of the sample. The spot size of the focusing laser light on the surface is about 100 ?m, and power density of the focusing laser light about 6 GW/cm^2. The radiation of the laser plasma was observed at a right angle to the laser beam with the use of an imaging quartz lens (f = 100 mm). The sample was placed in a small, vacuum-tight metal chamber (75 mm X 75 mm X 75 mm), which could be evacuated with a vacuum pump, and which was filled with the desired surrounding gas. The chamber pressure was measured precisely with a digital Pirani gauge (Diavac Ltd., model PT-1DA). Gas flow through the chamber was regulated by a needle valve in the gas line and a valve in the pumping line. For all experiments, the air pressure inside the vacuum was maintained at 1 Torr. The sample, together with the entire chamber and focusing lens, could be moved in the y-direction relative to the laser beam by means of a step motor and, in the x-direction via a micrometer screw. In addition to the window for transmitting the laser radiation, two optical windows were positioned around the laser plasma for visual and spectral observations. The windows were sufficiently large to ensure that plasma light was not obstructed by the walls when the position of the chamber was moved.

When no shock wave plasma was observed, the orange color incandescent emission light was imaged 1:1 by the quartz lens (f = 100 mm) with an aperture of 7 mm X 7 mm onto the plane of the entrance of two optical fibers which centers were separated by a distance of 6 mm. The exit of the fibers was then sent to each photomultiplier (Hamamatsu IP28) and photocurrents from the photomultipliers were then sent directly to different channels of a digital sampling storage scope (HP 54600B) after passing through a 500? resistance. The synchronization signal for the digital sampling storage scope was regulated by the external trigger function of the laser system. The velocity of the entities which induces incandescent emission was measured by reading the time difference in the rising time of each emission signal by varying the position of the combined fibers.

When the shock wave plasma was produced after the laser beam reached the sub target, the plasma light was imaged 1:1 by the quartz lens with an aperture of 10 mm X 10 mm on the plane of the entrance slit of a monochromator (Spex, model M-750, Czerny Turner conFiguration, focal length 750 mm, grating 1200 grooves/mm blazed at 500 nm). The output of the photomultiplier (Hamamatsu IP-28) was then fed to a

digital-sampling storage scope (HP 54610B, 500 MHz) after passing through a low-impedance circuit.

When the emission spectra of the shock wave plasma and the incandescent light of the gushing particles were taken, a gated intensified photo-diode-array (PDA, Princeton IRY 700) was used and the synchronization signal was also regulated by the external trigger function of the laser system.

The sample used in this experiment was high-vacuum silicon grease which was painted on the sub target material issued in this experiment was mainly copper (Rare metallic, 4N, thickness 0.2 mm).

3.1.3. Results and Discussion

Figure 3.1 shows a series of photographs when a TEA CO_2 laser was irradiated on the silicon grease painted on the copper sub target at a reduced air pressure of 1 Torr, (a) for the first irradiation, and (b), (c) and (d) for the second, third and fourth irradiations at the same sample position. It can be seen in Figs. 3.1 (a) and 3.1 (b) that the laser light had not yet reached the hard sub target and, as a result, only the incandescent emission light can be seen. The orange-red color is supposed to be associated with the heated particles coming from the grease sample. In Fig 3.1 (c), the combination of the incandescent light and the bright laser plasma light can be seen. In Fig 3.1 (d) a characteristic plasma shape is observed, which can be attributed to shock wave plasma. The bright color is assumed to come from highly excited atoms. After the laser light reached the sub target, two or three shots of laser irradiation were effective in producing the shock wave plasma, and after that no plasma generation took place even though laser irradiation was repeated. This means that the grease layer at the focused point on the surface was completely removed by the laser irradiation.

Fig 3.2 shows the spectrum in the UV region obtained (a) when the laser radiation has not attacked the sub target and (b) when the laser radiation has attacked the sub target. These spectra were collected by single-shot irradiation using the gated mode with an exposure time of 100 ? s. It can be clearly seen that before the laser light reaches the sub target, no atomic emission line was observed in the spectrum but only a dark noise. The atomic emission observed in (b) is attributed mainly to Si atoms. We also confirmed the detection of a strong 288.1 nm emission line ($3p^{2\ 1}D$-$4s^1p^0$) whose
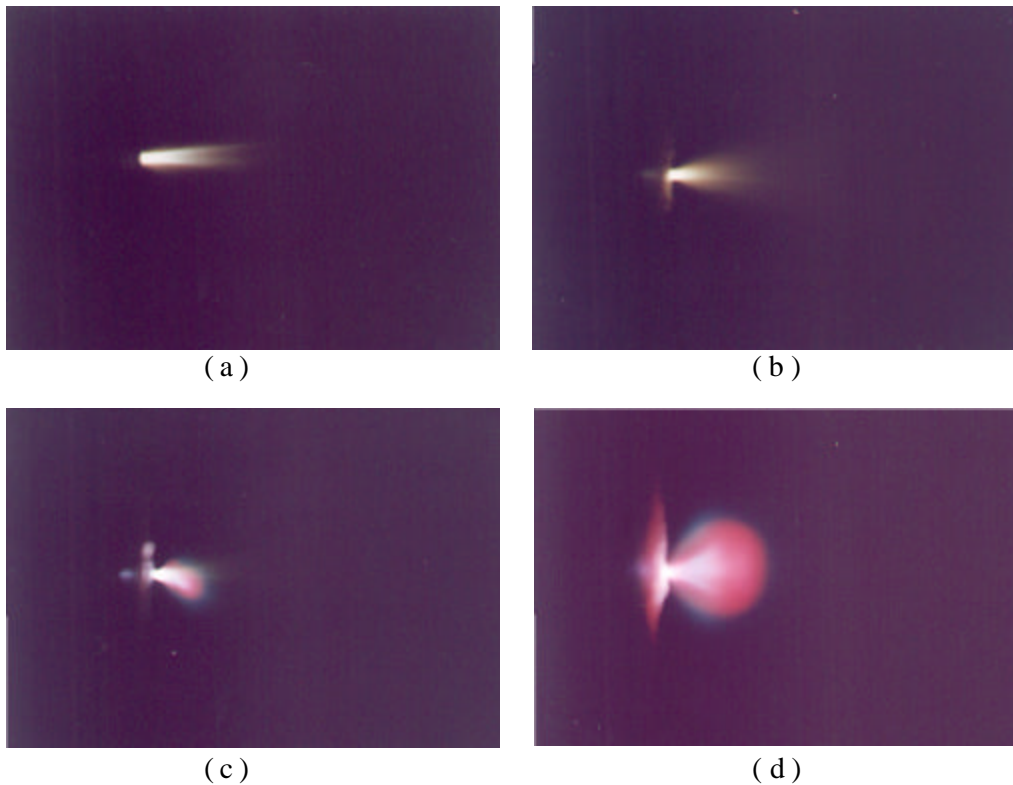
Fig 3.1. A series of silicon grease plasma photographs for (a) the initial application of laser radiation to the sample, (b), (c) and (d) the application of laser radiation for the second, third and fourth times to the sample surface at a fixed position

excitation energy is as high as 5.08 eV. Considering the strong emission from the excited state of Si, it is assumed that the temperature of the secondary plasma is more than several thousand degrees. According to our previous experiments on the shock wave plasma, the temperature was estimated to be around 8000ºK.[6,9)]

Here, it should be stressed that under careful microscopic investigation, crater formation and damage to the surface of the copper sub target were not observed after the laser bombardment in both cases, with the silicon grease and without the silicon grease. However, when we used brass as the sub target, a small crater was seen after successive laser irradiation. This is because the threshold of its high reflectivity (more than 90%) at around 10.6 ? m. From this result we can say that the secondary plasma consists of only silicon grease, and the copper plate plays the role of a repulsion substrate only, enhancing the speed of the gushing atoms and it is never evaporated.

(a)

(b)
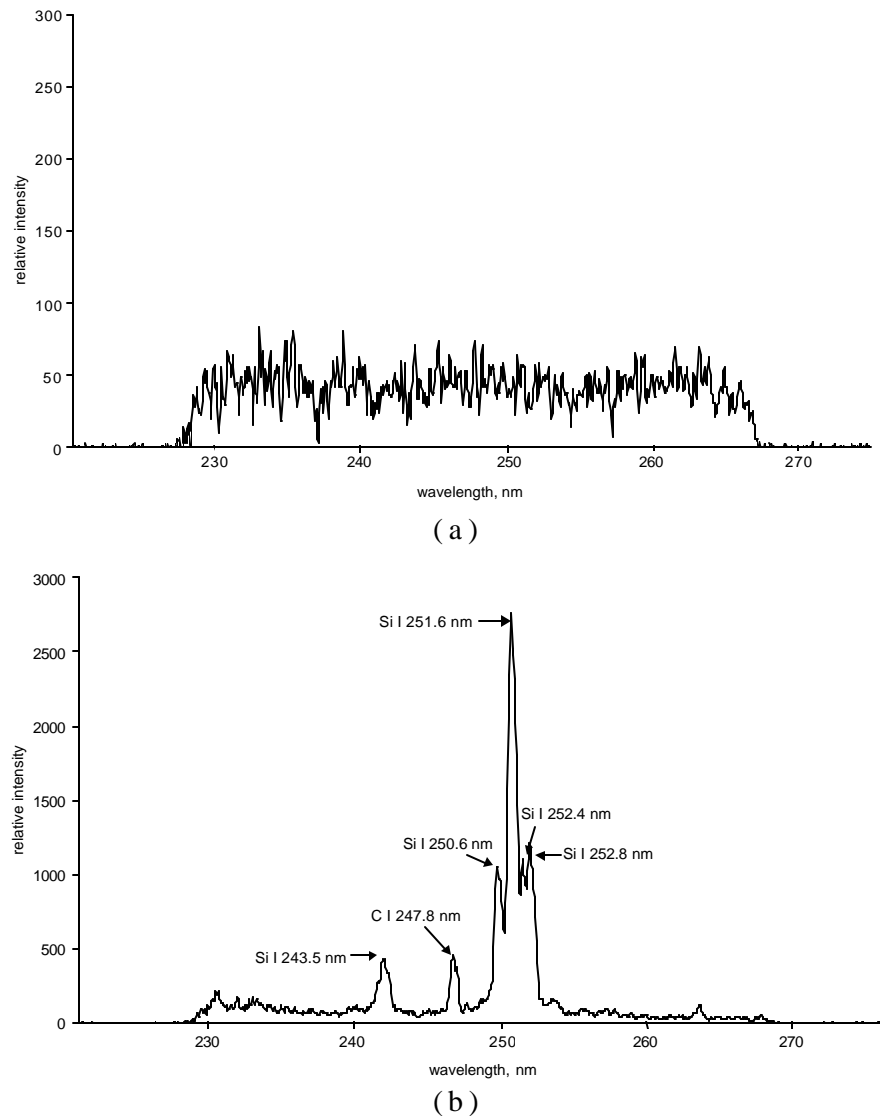
Fig 3.2. Spectrum of the silicon grease plasma in the UV region (a) when the laser radiation has not reached the sub target and (b) when the laser radiation reaches the sub target

Fig 3.3 shows the speed of the particles and the atoms gushing from the sample. It was found that, in the absence of a shock wave plasma, the speed of the incandescent light from the gushing particles were very low, less than Mach 7 and almost constant during transmission in the ambient gas. The signal was picked up using the continuous emission spectrum on the incandescent light with the aid of two fibers. The emission spectrum was examined in advance using the gated intensified PDA in the visible region. As a result only a week continuous spectrum was observed. From these results it is seen that the particles which gives emission are not light particles,

but rather weight particles or droplets because if they are light particles that speed would soon decrease due to collision with the ambient gas.
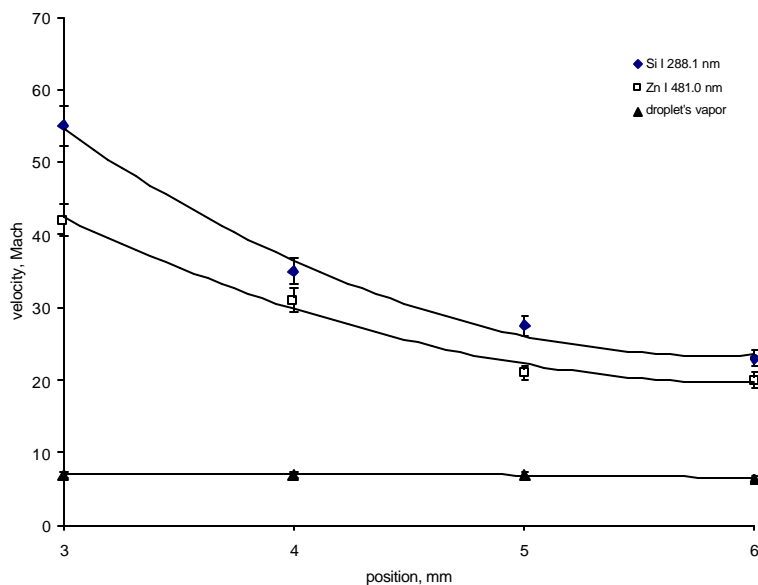
Fig 3.3. The relationship between the velocity of the Si I 298.7 nm, Zn I 481.0 nm and incandescent light as a function of plasma position

The velocity and time position can be calculated as follows:

$$\frac{? \ starting \ point \ of \ two \ signals}{length \ of \ 1 scale \ time \ setting} ? \ time \ setting \ ? \ time \ propagatio \ n \ (?s)$$

$$\frac{distance \ between \ two \ fibers}{time \ propagatio \ n} ? \ velocity \ (Km/s)$$

$$\frac{velocity}{sound \ propagatio \ n \ in \ air} ? \ velocity \ (Mach)$$

When a shock wave plasma was generated, the speed of the silicon atoms was measured using Si I 298.7 nm and was as high as Mach 55 near the target (3 mm), decreasing to Mach 30 at 6 mm above the sample surface. These data were derived from the result of the relationship between the slit position and the rising time, which was obtained by varying position of the chamber together with the focusing lens, as mentioned in the previous section. The time profile as the function of position is shown in Fig 3.4. In order to compare the result of Si plasma with ordinary laser-induced metal plasma, we used brass sample as the target without grease. The curve is shown in Fig 3.3.

Fig 3.5 shows the relationship between time and the displacement distance of the front of the emission which was observed by reading the rising point of the secondary plasma. It can be clearly seen that, for the both cases, the slope is near 0.4 which is
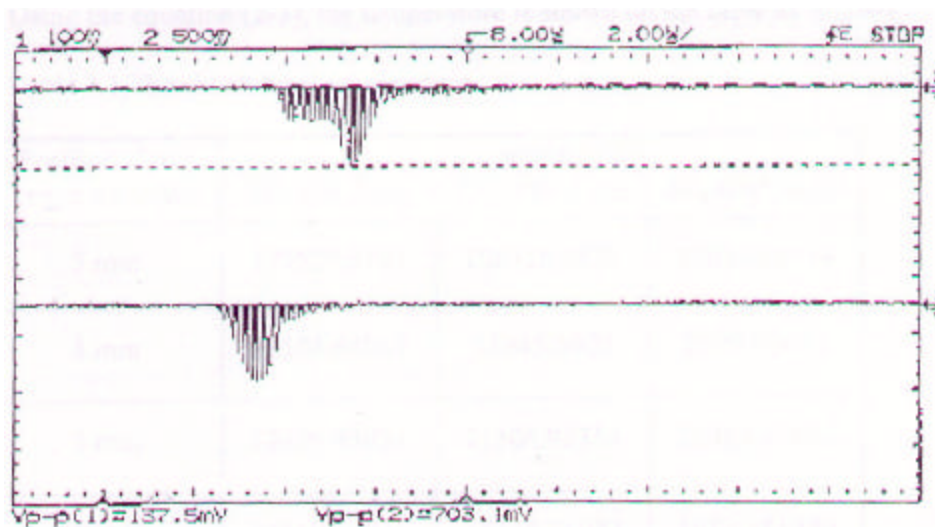
Fig 3.4. Incandescent light's time profile as the function of position
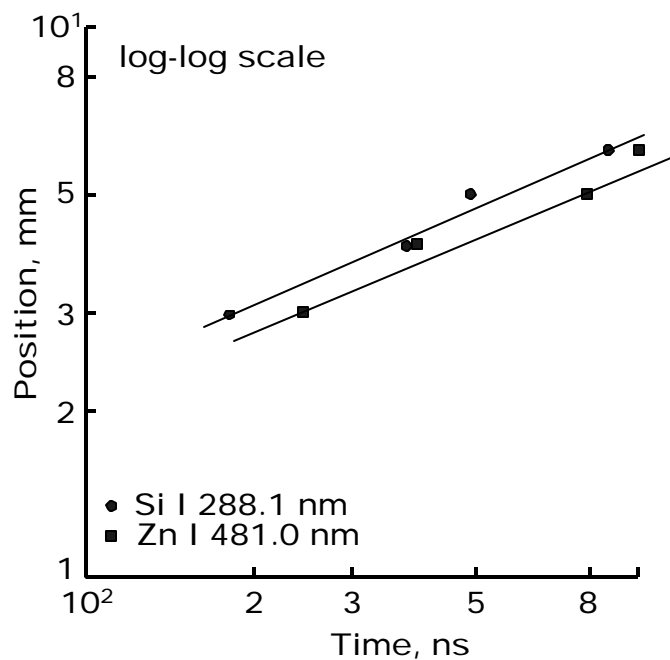
Fig 3.5. The relationship between the time and the distance of the rising point of emission of Si I 298.7 nm and Zn I 481.0 nm at 1 Torr surrounding air in log-log plot

good with the agreement with the theoretical result derived by Sedov for the blast wave.[21] Based on these experimental facts we have already proved that the zinc plasma can also be produced even in the soft material when the suitable sub target is placed at the back of the sample.

In addition to these experiments another experiment was performed. Namely $CuSO_4.5H_2O$ powder was mixed with silicon grease in several weight percentages. The grease containing $CuSO_4.5H_2O$ was painted on the copper sub target, and irradiated in the same manner as described above. As the result, a similar result was observed; namely, no secondary plasma was observed at the beginning of the shots of laser irradiation, but after the laser light reached the target very bright secondary plasma was observed with a nearly hemispherical shape after a few shots of laser irradiation. The secondary plasma emitted very bright green emission due to Cu atoms in $CuSO_4.5H_2O$. Therefore, it can be said that this sub target technique can be applied to the spectrochemical analysis of powder samples; in general, such powder samples can not be used as a sample for laser ablation atomic emission spectrometry.

It is assumed that when the surface of the target is soft, the expulsion of atoms by the surface is weakened because the softened surface absorbs the recoil energy and the atoms gushing from the primary plasma do not acquire sufficient speed to form a shock wave. On the other hand, when the hard sub target is placed on the back in tight contact with the sample, the forward momentum of the gushed atoms does not weaken without absorbing the energy. We have already proposed the model to explain the generation of shock wave plasma.[6,9)] Namely, by the action of atoms gushing from the target, the induced adiabatic compression of the surrounding gas creates a shock wave. As a result of the compression, the kinetic energy of the propelled atoms is converted into heat energy in the plasma.

The sub target effect was also confirmed on a phosphor low-melting-point glass. As reported in the previous work, shock wave plasma could not be generated when a TEA CO_2 laser (300 mJ) was focused on a phosphor low-melting-point glass with a power density of 0.6 GW/cm^2, while under the irradiation of XeCl laser, a shock wave plasma was produced.[8)] We have checked the sub target effect on the phosphor low-melting-point glass using the previous TEA CO_2 laser. As a result good shock wave plasma was observed when we set a metal sub target on the back of the glass. Namely, before the laser beam penetrated the target, only jet-like orange color emission was observed. However, after several laser shots of irradiation the bright hemispherical plasma appears suddenly when the laser beam attacked the sub target directly, and the atomic emission assigned to phosphor was clearly observed.

Another experiment was performed to confirm the sub target effect on a pellet which was made by compressing KI powder mixed with tea leaf powder. The purpose

of this experiment was to perform a quantitative analysis of the F element in the tea leaf. In order to increase the detection sensitivity, we increased the amount of tea leaf powder content in the pellet. In such a case the pellet hardness was extremely degraded, and it became difficult to produce a shock wave plasma because of the lack of repulsion force on the surface of the sample. However, when we set the sub target on the back of the pellet, bright secondary plasma was produced after the laser beam penetrated the pellet, and the generation of the bright secondary plasma was observed. By this method, we succeeded in detecting F in the tea leaf using several ionic emission line of F, such as F II 350.5 nm and F II 384.7 nm.[22] Therefore, we can say that the sub target effect can be effectively employed for practical application in the quantitative analysis of soft samples.

3.1.4. Conclusion

It has been proved that in the case of soft samples, such as silicon grease shock wave plasma cannot be produced. However, when we placed a sub target on the back of the sample, shock wave plasma is generated. It is believed that in the absence of a sub target, the expulsion of atoms is weakened because the soft surface absorbs recoil energy, and atoms gushing from the primary plasma do not acquire sufficient speed to form a shock wave. The main role of the sub target is to produce a repulsion force for atoms gushing with high speed. That experimental results obtained in this study are also strong evidence that support our shock wave model which explains the mechanism of laser-induced shock wave plasma. It should be noted that this sub target method can be successfully utilized to realize highly sensitive and rapid quantitative analysis of soft sample, such as grease and biological samples.

3.2. Sub Target Effect on Laser Plasma Generated at Atmospheric Pressure

3.2.1. Introduction

In this experiment, we prove that even at 1 atm the shock wave model can well explain the generation of the laser plasma. Thus, the characteristics of the laser plasma obtained at this atmospheric pressure were then analyzed based on our shock wave model proposed for low-pressure laser plasma, and the results showed that the excitation mechanism of LIBS is essentially the same as that our shock wave model. It is therefore believed that the breakdown mechanism did not play a crucial role in the generation of atmospheric laser plasma. Initial quantitative analysis for elemental calcium of water from the blow-off of a boiler system was also carried out.

3.2.2. Plasma Ge neration in Surrounding He at Atmospheric Pressure

The experimental arrangement used here can be readily seen in Fig 3.6. In this experiment, laser irradiation from a 10.6 ?m TEA CO_2 laser (Lumonics, multigas laser, model HE440) was operated shotwise, and the laser output energy was fixed at 100 mJ. The laser beam was focused by a ZnSe lens (f = 100 mm) through a ZnSe window onto the surface of a sample.
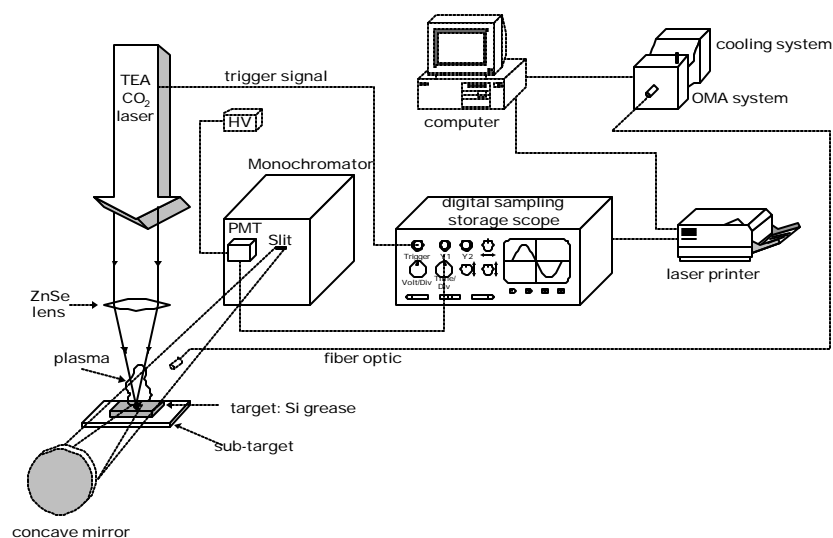
Fig 3.6. Diagram of experimental setup for this experiment

The sample was placed in a metal chamber (75 mm X 75 mm X 90 mm) could be evacuated with a vacuum pump and filled with the desired gas up to a certain pressure. Chamber pressure was measured precisely by a digital manometer (Diavac

PT-1DA). Gas flow through the chamber was regulated by a needle valve in the air line and another valve in the pumping line. The sample, together with the entire chamber and the ZnSe lens, could be moved in two directions with the use of a step motor for movement in the laser beam direction. The sample was fixed at the same position during irradiation.

The radiation of the laser-induced plasma was observed through an optical window at right angles to the laser beam by means of an imaging quartz lens (f = 100 mm) with an aperture 10 mm X 10 mm. The plasma was imaged with an enlargement (1:3) onto the entrance slit of a monochromator (Spex M-750, Czerny Turner configuration, focal length 750 mm, grating of 1200 grooves/mm blazed at 500 nm). The entrance slit was set at 2 mm in height and 100 ?m in width so that the observation area could be restricted to the limited region. The electric signal output from a photomultiplier (Hamamatsu IP-28) was fed through a time-resolved circuit (its RC time constant was 30 ns) into the first channel of a digital sampling storage scope was obtained from the trigger output of the laser system.

When emission spectral data were taken, a gated intensified photo diode array (PDA, Princeton IRY 700) with 700 sensitized channel was used and the synchronization signal was regulated by the external trigger function of the laser system. The sample used in this experiment was high-vacuum silicon grease which was painted on the sub-target surface with a thickness of roughly 100 microns. The sub-target material used in this experiment mainly copper (Rare Metallic Co. 4N, thickness of 0.2 mm). When quantitative analysis of water was carried out, water from the blow-off of a boiler system which contained calcium was used. The water (50 cm^3) was then allowed to evaporate and the remaining solid was collected by using silicon grease.

3.2.3. Results and Discussion

A TEA CO_2 laser was accurately focused on silicon grease samples painted on the copper surface as a sub-target in a surrounding air of 1 atm. At the first irradiation, the laser light had not yet reached the hard sub-target and, as a result, the sound from the explosion was very weak until the fourth shot. For the fifth shot, the laser light was assumed to have reached the sub-target set in the back surface of the silicon grease samples, and at this point, a loud sound due to the generation of shock waves

could be clearly heard. The plasma was cone-shaped with a diameter around 4 mm in the case of surrounding air at 1 atm. In the case of helium at 1 atm, the plasma size was smaller than that in air at the same laser energy. It should also be noted that helium emission lines could be readily observed compared to air, and this was why we used helium in all of our experiments. Here, it should be stressed that careful microscopic investigation revealed no crater formation on or damage to the surface of the copper sub-target after laser bombardment in either case with and without the silicon grease. On the basis of these results, we can say that the laser plasma consists of only silicon grease, and the copper plate plays the role of a repulsion substrate only. Namely, it is considered that when the surface of the silicon grease is soft, the expulsion of atoms is weakened because the soft surface absorbs the recoil energy and the atoms gushing from the silicon grease is not weakened because the copper plate acts as a wall on which atoms are reflected.
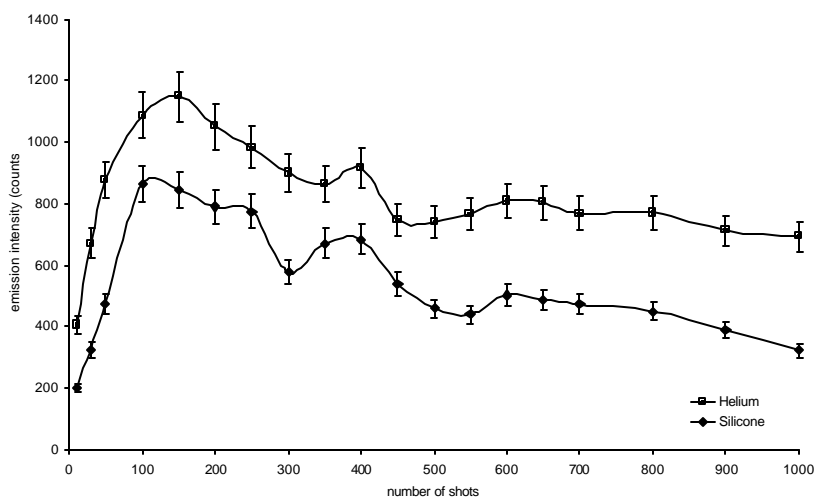
Fig 3.7. Time and spatially integrated emission intensity of Si I 288.1 nm and He I587.5 nm as a function of the number of laser shots at a fixed position. Data were taken in surrounding helium gas of 1 atm

In order to examine how the emission intensity of He I 587.5 nm and Si I 288.1 nm varies with the number of repeated laser irradiation at a fixed position, we investigated the effect of laser bombardment on a silicon grease target on copper plate in the presence of helium gas at 1 atm. Figure 3.7 shows that the emission intensity could not be found at the initial laser bombardment but after five shots, the emission intensity appeared for both helium and silicon and increased rapidly up to 200 laser shots, after which it more or less became constant and then decreased with the further increase in the number of laser shots to 1000. It should be noted that in our previous

work conducted at reduced pressure in air, only the third and fourth shots produced shock wave plasma and thereafter the plasma disappeared because the laser light already reached the surface of the sub-target. It is therefore considered that in the high-pressure case, the silicon grease around the laser focal point, melted during the repeated laser irradiation and the flow grease were then directed to the laser focal point, yielding almost a constant emission intensity of the silicon lines.
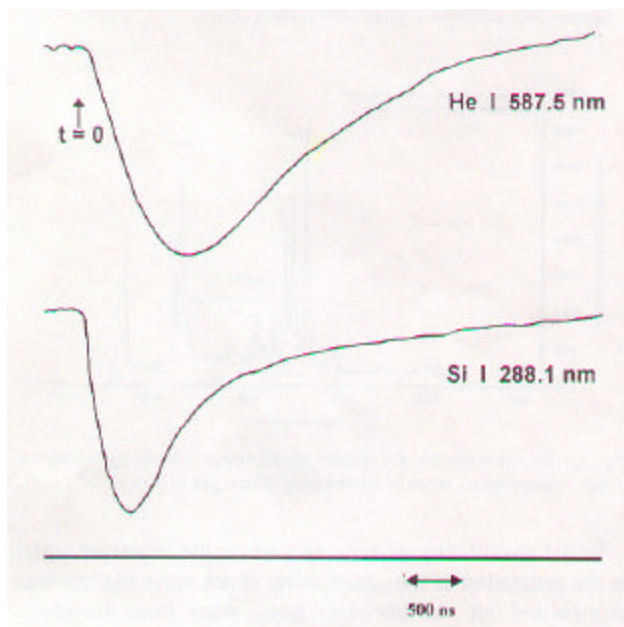
Fig 3.8. Time profiles of the emission intensity of Si I 288.1 nm and He I 587.5 nm observed at 1.3 mm in helium at 1 atm

Figure 3.8 shows the time profiles of the emission intensity of Si I 288.1 nm and He I 587.5 nm observed at 1.3 mm under helium gas at 1 atm. Both curves show a similar pattern consisting of two components: one is a steep climb observed at the early stage of plasma irradiation and the other is the decline at a slower pace. These emission characteristics are considered to correspond to the shock excitation stage and the cooling stage, respectively, which have been proposed to explain laser plasma generation at low pressures; namely, the steep climb is related to the process of continuous compression of the gushing atoms. It has been proved in our previous studies.[6,35] that the life time of the primary plasma is about twice that of the laser pulse width (FWHM = 50 ns), and within the time, most of the atoms gush out from the primary plasma at high speed. At the beginning of the expansion, the temperature of the atom cluster gushing out from the primary plasma is relatively low. With time, the compression proceeds and intensifies. Consequently, the plasma temperature rises

to enhance the atomic emission. This process takes place in the shock excitation stage. Soon afterward, the cluster of atoms begins to slow down while losing its energy to the surrounding gas. As a result, no further excitation will take place, since the compression between the shock front and the propelling atoms can no longer be sustained due to the increasing separation between them, while the cluster of atoms continues to move forward with its residual momentum. Since the surrounding gas behind the shock wave is left with high temperature, and the secondary plasma also contains a large amount of residual thermal energy, the cooling of the plasma is bound to proceed slowly with time. We call this part of the process the cooling stage. It should be noted that the rising point of helium emission comes later than that of silicon emission. This means that the breakdown mechanism did not play a crucial role in the atmospheric plasma generation and therefore, by compressing of the atoms gushing from the target, the surrounding gas was excited.
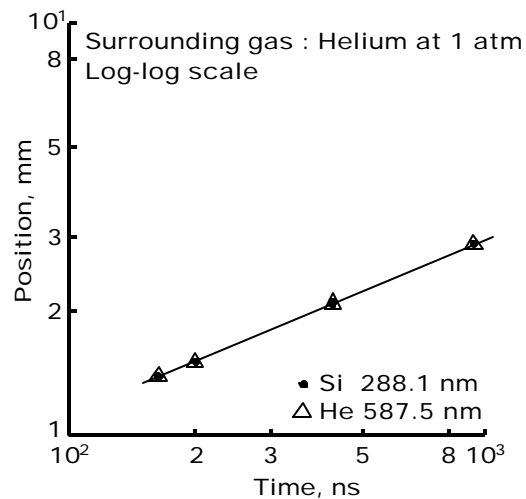
Fig 3.9. Relationship between the propagation length of the secondary plasma front and helium atoms as the function of time

In order to complete the elucidation of the excitation mechanism of the secondary plasma and the surrounding gas atoms, one also needs to know how the front of the secondary plasma and He emission moves with time. This key information on the propagation of the secondary plasma and He emission is provided by the data depicted in Fig 3.9. The plot consists of one linear segment with a slope of 0.4. It should be noted that the fronts of the Si emission and He emission share the same position in curve. This means that Si atoms and He emission move with the same speed; namely, Si atoms function as a piston in compressing the surrounding helium

gas, yielding the emission of helium atoms. The slope of 0.4 exactly supports the shock wave model proposed by Sedov.[21]

Initial quantitative analysis to confirm the sub target effect in the generation of the atmospheric shock wave plasma was also carried out. In this experiment, water from the blow-off a boiler system was used. This water, which contained calcium, was then evaporated and the residual solid was collected with the silicon grease which was then painted on the copper surface. Figure 3.10 shows the emission spectra taken using the OMA system. From the spectra we can clearly see the appearance of Ca II 393.3 nm and Ca II 396.8 nm. The detection limit in this experimental stage was estimated from the signal to noise ratio in the emission spectra in Fig 3.10, to be around 5 ppm for calcium in natural water. It is expected that this detection limit will be much lowered by increasing the energy of TEA CO_2 laser, because in this experiment we used the TEA CO_2 laser with a relatively low pulse energy.
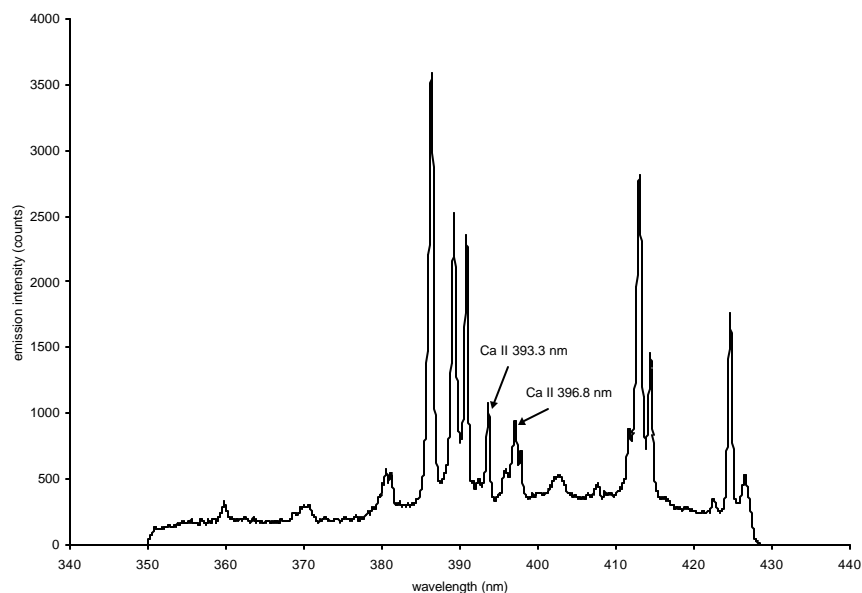
Fig 3.10. Emission spectra of a silicon grease sample containing calcium at low concentrations, taken in surrounding helium gas of 1 atm

3.2.4. Conclusion

It has been proved that in the case of soft samples, such as silicon grease, a shock wave plasma cannot be generated. However, when we place a sub target on the back surface of a sample, a shock wave plasma is generated followed by the loud explosion sound. It is believed that in the absence of a sub target, the expulsion of atoms is

weakened because the soft surface absorbs recoil energy, and atoms gushing from the primary plasma do not acquire sufficient speed to form a shock wave. The main role of the sub target is to produce a repulsion force for atoms gushing with a high speed. The experimental results showed that the mechanism of laser-induced breakdown spectroscopy (LIBS) is essentially the same as that proposed in our LISPS model. It is then believed that the breakdown mechanism did not play a crucial role in the generation of atmospheric laser plasma. Further experiments are being undertaken in order to apply sub target effect in spectrochemical applications in high-pressure surrounding gas, and the results will be reported elsewhere in the near future.

Chapter Four

CONFINEMENT EFFECT IN QUARTZ SAMPLE

4.1. Confinement Effect in Enhancing Shock Wave Plasma Generation at Low Pressure by TEA CO_2 Laser Bombardment on Quartz Sample

4.1.1 Introduction

In performing laser microprobe analysis, repeated irradiation is usually directed to a fixed position on the sample surface. Consequently a micro crater will be created on the sample surface, which deepens as the shot number increases. We have observed in a preliminary experiment using a TEA CO_2 laser irradiated on a quartz sample that the depth of the crater was intimately related to the so-called pre-irradiation effect at the first few shots, characterized by the generation of primary plasma without being followed by the appearance of the secondary plasma as normally observed on metal samples. Only after a number of shots, when the crater has reached a certain depth, did the secondary plasma begin to develop in concurrence with the generation of the primary plasma. Since the formation of secondary plasma is a crucial condition for the application of LISPS, the effect of the crater must be thoroughly investigated and understood before the analytical method can be properly applied to this and similar samples. Recently, there appeared some papers in which crater characteristics were discussed with regard to laser ablation process.[23,24] However, to the best of our knowledge, no report has been published on the laser plasma confinement effect arising from the crater. The aim of this experimental work is to produce a clear description of the pre-irradiation phenomenon in relation to the influence of the crater. This will in turn be studied in terms of its confinement effect on the primary as well as secondary plasmas generated from quartz samples at reduced surrounding gas pressure. It will be shown that the correlation between those effects can be understood on the basis of our shock wave model.

4.1.2. Experimental Procedure

The complete experimental setup is described in Fig. 4.1. In this experiment, the 10.6 ?m TEA CO_2 laser (Shibuya Kogyo, SQ-2000, 3J, 100 ns) was operated shot to shot with the laser output energy varied from 500 mJ to 800 mJ by using the appropriate apertures. The laser beam was focused by a Ge lens (f = 100 mm) through a ZnSe window onto the sample surface. The sample was placed in a vacuum tight metal chamber measuring 125 mm x 100 mm x 100 mm. This chamber was evacuated with a vacuum pump and filled with the desired gas up to a certain pressure, which was measured and monitored by a digital manometer (Nishiyama Seisakusho, DM-760). Gas flow through the chamber was regulated by a needle valve in the air line and another valve in the pumping line. The sample, together with the entire chamber and the Ge lens, could be moved in two directions by the use of a step motor for movement in the laser beam direction and a micrometer for movement perpendicular to the laser beam direction. The sample was fixed at the same position during irradiation, while the emission intensifies of the plasmas were detected through an optical window of the chamber at right angle to the laser beam.
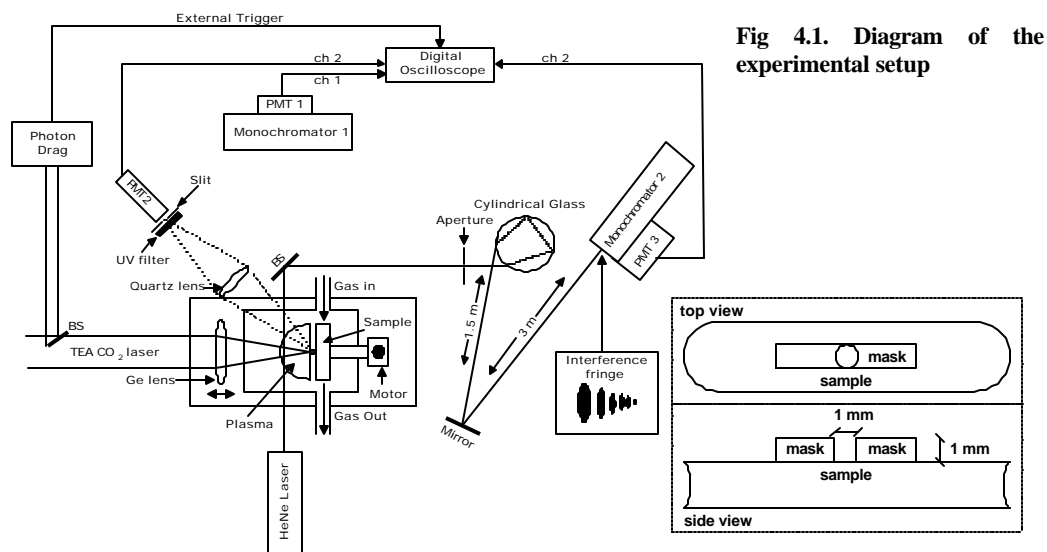
Fig 4.1. Diagram of the experimental setup

For the study of pre-irradiation effect, a time-evolution measurement was performed on the spatially integrated emission intensifies of both the primary and secondary plasmas. In the measurement of the secondary plasma emission, the monochromator was set for the wavelength of Si 1 288.1 nm with the position of the entrance slit fixed at the center of the secondary plasma without using lens, so that the

entire emission of the plasma was collected directly by monochromator 1. Meanwhile for intensity measurement of the primary plasma, an imaging quartz lens (f = 40 mm) was placed outside the chamber at a position making an angle of around 60° with the beam direction. As indicated in the figure, this arrangement allows the primary plasma to be imaged 1:1 onto the entrance slit in front of photomultiplier 2 Hamamatsu R585). This slit was set at 2 mm in height and 2 mm in width behind a UV band pass filter (UV D36B), so that only the image of the primary plasma was detected by photomultiplier 2. The electric signals from two photomultipliers were separately fed through a 500 k? resistor to the digital scope. In this experiment, different surrounding gases were employed to study their different effects. The plasma radiation of the primary plasma is detected by an optical multichannel analyzer (OMA system, Atago Macs-320) attached to a monochromator with a focal length of 320mm and connected to an optical fiber. Additionally, an investigation was conducted on the confinement effect caused by the presence of a hole in a metal mask as well as that due to the crater created on the sample. In an effort to explain the physical origin of the pre-irradiation phenomenon, the crater effect and the related confinement effect were examined in connection with the generation of shock wave, which is supposed to be responsible for secondary plasma generation. To this end, a unique density jump detection method using rainbow interferometer[13,25,26] was adopted. In this method, a He-Ne laser light was sent perpendicular to the TEA CO_2 laser beam into the expansion region of the laser plasma as depicted in Fig. 4.1. The outgoing probe beam was sent into a cylindrical glass (60 mm in diameter) in such way that the laser light undergoes minimum deviation. Under this condition, the beam emerging from the cell exhibits a fine interference fringe pattern. It should be stressed that using this equipment, the interferometric experiment could be carried out without the use of an additional and delicate amplitude splitting setup. In this experiment, the second order fringe series of the rainbow interference was chosen for the detection of density jump. The separation between adjacent fringes in this series is about 0.5 mm. The slit of monochromator 2 (0.1 mm) was set at the middle point between the minimum and the peak of the second fringe for detecting the shift of the fringe when a shock wave arrives at the probing area. The signal coming from photomultiplier 3 (Hamamatsu R585) attached to monochromator 2 was fed into the second channel of the digital storage scope through a 500 ? resistor. In all the measurements the digital storage

scope was triggered by a fraction of the TEA CO_2 laser beam using a photon drag detector (Hamaphoto B749).

4.1.3. Results and Discussion

It is found in these experiments that the primary and secondary plasmas generated from quartz sample have distinctly different threshold energies. While the threshold energy for primary plasma generation is 500 mJ, no secondary plasma was observed even after 50 shots when the laser energy was set lower than 638 mJ. On the other hand, at laser energy higher than 638 mJ, for instance 758 mJ, the secondary plasma is found to be generated along with the primary plasma right from the first shot.

(a)   (b)
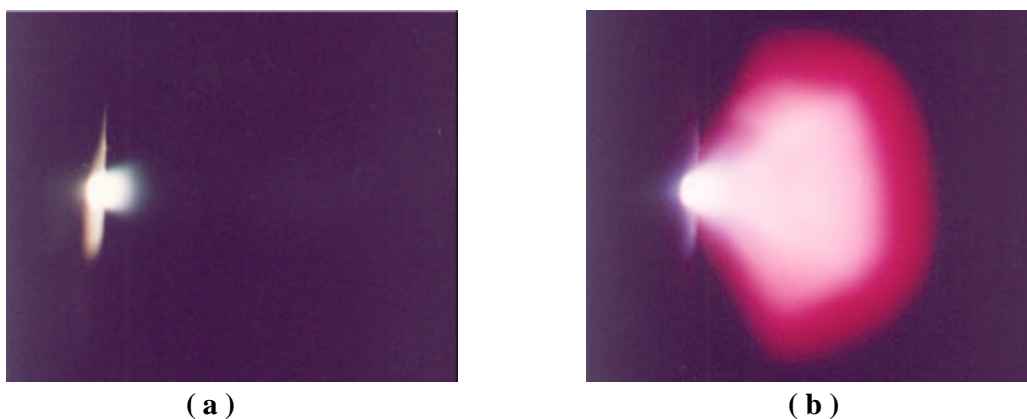
Fig 4.2. A plasma picture taken by irradiating a quartz sample using a TEA CO_2 laser of 550 mJ energy (a) at the first irradiation, only the primary plasma can be seen in this picture and (b) after 25th repeated irradiations in which the secondary plasma could clearly observable

The pre-irradiation effect observed in this experiment with 550 mJ laser energy is illustrated by the two photos presented in Fig. 4.2. Fig. 4.2(a) shows the primary plasma generated at the first shot of irradiation. The secondary plasma is ostensibly absent in the picture. As the crater created on the sample surface deepens after repeated shots of irradiation, the secondary plasma becomes fully developed around the primary plasma as shown in Fig. 4.2(b). This observation is further corroborated by the result of intensity measurement given in Fig. 4.3. There are two important features to be noted in this figure. One is the delayed occurrence of the secondary plasma at the tenth shot, although the primary plasma is already observable at the first shot. The other feature is indicated by a sharp rise of the primary plasma intensity after about 45 laser shots accompanied by a relatively milder increase of the secondary plasma intensity. The delayed formation of the secondary plasma may be

attributed to several possible effects such as the preheating effect, radiation induced changes of optical and physical properties or the confinement effect due to the crater created by repeated irradiations. Clarification of the roles of these effects will be given in the following analysis of the additional experimental data.
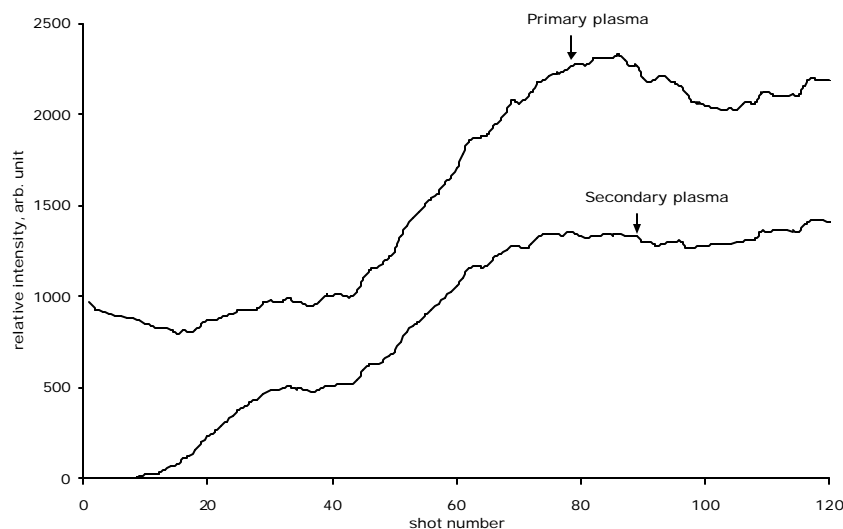
Fig 4.3. The relationship between the occurrence of emission intensity of primary plasma and secondary plasma as a function of laser shot number on quartz sample. The TEA CO_2 laser energy was set at 550 mJ and using an air at 2 Torr as a surrounding gas

In order to examine the preheating effect, the laser irradiation was stopped after the secondary plasma was produced. The presence of crater was clearly visible in this case. Soon after the sample surface had cooled down, the irradiation was resumed and directed at the same position, and no pre-irradiation effect took place. In other words, both primary and secondary plasma were produced from the first irradiation. This result clearly eliminates the role of preheating effect in the generation of secondary plasma. We are thus left with the other two possible effects.

These possibilities are investigated by using an aluminum plate measuring 1 mm in thickness, which contains a hole with a diameter of 1 mm. This plate was used as a mask in front of the new and unirradiated sample surface. Since the depth of the crater formed after 100 shots is about 1 mm, the thickness chosen for the plate is certainly appropriate to demonstrate the confinement effect of the crater. The laser irradiation was then passed through the hole of the mask. It is found once again that both primary and secondary plasmas could be generated at the first shot as clearly indicated in Fig.

4.4. This result further eliminates the possible effect of radiation-induced changes of optical and physical properties. This leaves us with the sole effect of plasmas confinement due to the presence of the hole in the mask or the crater created by repeated irradiation prior to the generation of secondary plasma.
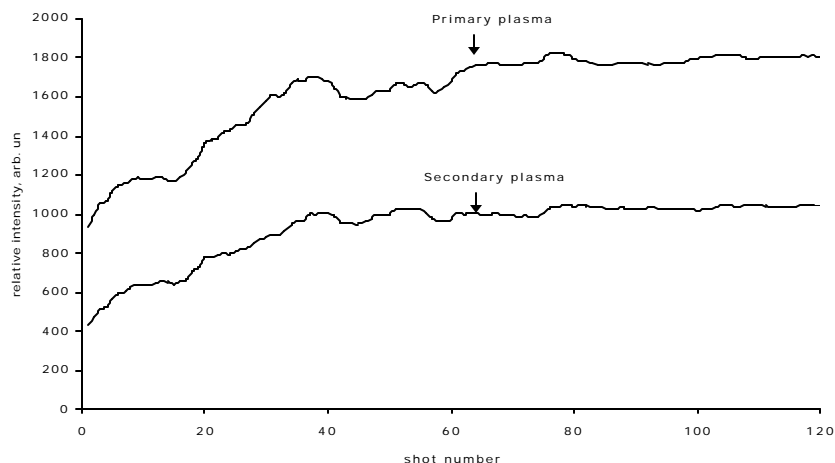
Fig 4.4. The relationship between the occurrence of emission intensity of primary plasma and secondary plasma as a function of laser shot number on quartz sample. An aluminum mask with a diameter of 1 mm and thickness of 1 mm was put in front of the quartz sample. The TEA CO$_2$ laser energy was set at 550 mJ and using an air at 2 Torr as a surrounding gas

In our previous experiment, we have already proposed the shock wave model to explain the generation of secondary plasma. Namely, a shock wave is created by the adiabatic compression of the surrounding gas induced by the action of atoms gushing out from the target. The secondary plasma is in turn generated by the shock wave. As a result of the compression, the kinetic energy of the propelled atoms is converted into thermal excitation energy in the plasma. Obviously, ablated atoms with less energies will lead to an ineffective compression process and hence unfavorable condition for the generation of shock wave required for the formation of the secondary plasma.

It is understood on general ground that the confinement of plasma formation region will lead to the enhancement of primary plasma and the suppression of energy dispersion. Both of these effects are expected to result in higher gushing speed of the ablated atoms, and hence more favorable condition for the formation of shock wave responsible for the generation of secondary plasma and therefore the elimination of pre-irradiation effect. This suggested effect of the crater was confirmed by the detection of density jump with the experimental setup described in Fig. 4.1 which was explained in our previous papers.[13,25,26] It was found that no significant signal of

density jump was observed at the initial shots of laser irradiations. A sharp density jump showed up as soon as the secondary plasma became clearly visible in conjunction with the appearance of a crater. This observation establishes the role of the crater in giving rise to the confinement effect, which results in the enhancement of shock wave formation. This shock wave plasma generation mechanism also explains naturally the absence of pre-irradiation effect at higher laser energies.
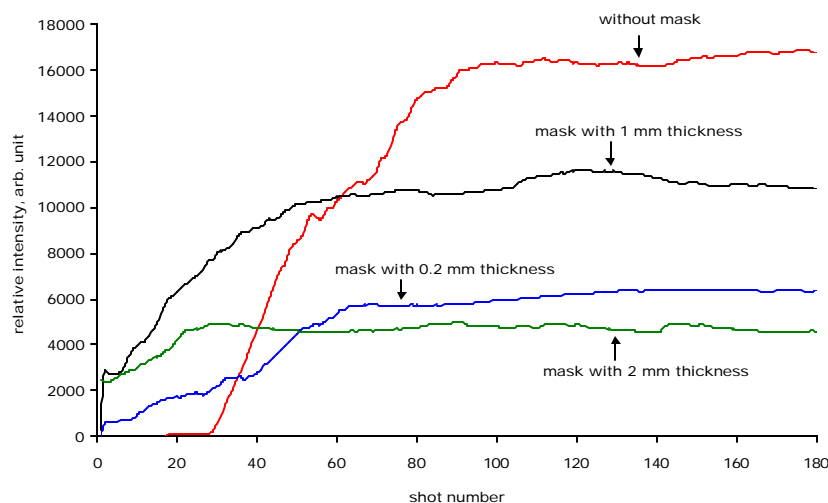
Fig 4.5. The relationship between the secondary plasma emission intensity and laser shot number for different mask thickness. The TEA CO$_2$ laser energy was set at 550 mJ and using an air at 2 Torr as a surrounding gas

The effect induced by the crater was further investigated by simulating it with aluminum masks of various thickness (0.2 mm, 1 mm and 2 mm), each containing a hole with diameter of 1 mm. The result of secondary plasma emission measurement is presented in Fig. 4.5. It clearly shows that the presence of the mask reduces significantly the pre-irradiation effect even with a thickness of 0.2 mm, and eliminates the effect completely when thicker masks are used. The presence of a hole on the irradiated surface is thus indicative of the occurrence of confinement effect, which enhances the formation of the secondary plasma. In all cases, the plasma intensity always undergoes initial growth and more or less stabilizes henceforth. The general suppression of intensity upon the introduction of a mask on the sample surface is also clearly visible. The intensity reduction is most likely due to less effective thermal excitation process in the hole as heat is more readily diffused by the metal mask. The intensity variation with respect to thickness of the mask can be explained as follows. In the case of the thinnest masks (0.2 mm), the wall of the hole is simply not deep

enough to enhance effectively the compression process needed for the shock wave generation. The considerably higher intensity produced with the mask of 1 mm thickness clearly attest to a stronger confinement effect. The pronounced drop of intensity caused by doubling the mask thickness may, on the other hand, due to the ineffective delivery of laser power to the sample surface. In other words, given the size and the depth of the hole in the mask, the laser beam failed to pass through the hole freely without suffering from undesirable energy loss to the wall. A larger size of the hole would have overcome this problem, but only at the expense of reducing the confinement effect required to prevent the pre-irradiation phenomenon. It appears from this experiment that a hole size of 1 mm diameter for a laser beam of 0.5 mm beam waist, and a hole depth of 1 mm are more or less the optimal trade-off between the two counter acting effects of plasma confinement and reduced energy delivery. This analysis also helps to explain the trend toward stabilization the intensity growth after a large number of shots, when the two competing and opposite effects attain a state of equilibrium as the crater deepens. The earlier attainment of this state with deeper holes is a further verification of this working mechanism.
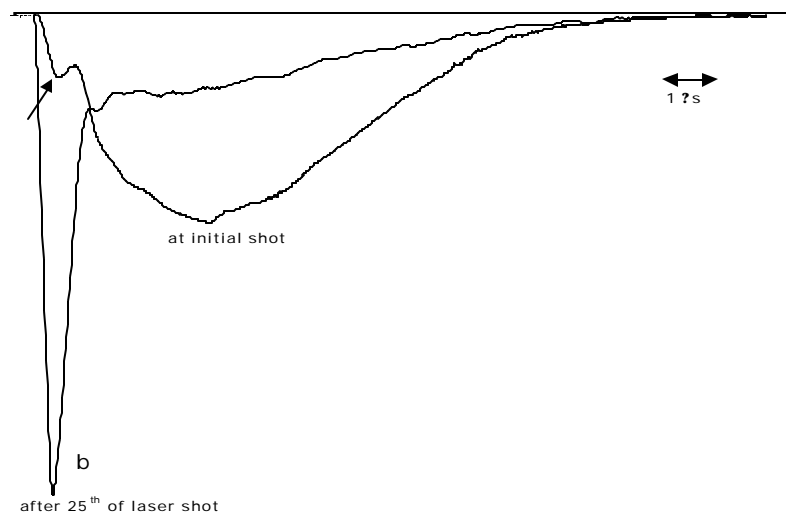
Fig 4.6. Time evolution of the primary plasma emission intensity at (a) for the initial shot and (b) for after 25th repeated shots without using an aluminum mask. The TEA CO$_2$ laser energy was set at 550 mJ and was focused onto quartz sample at surrounding air pressure of 2 Torr

To complete the picture on the confinement effect, a time profile measurement of the intensity evolution of the primary plasma was carried out employing the set-up for secondary plasma measurement without the lens and with the 500 k? resistor replaced by a 500 ? resistor. The result presented in Fig. 4.6 consists of the time

profile measured at the first shot and another one at the 25th shot, all taken without the mask. Although the time integrated emission intensity of the primary plasma taken at the first shot roughly is the same with that obtained at the 25th shot as shown in Fig. 4.3, the associated time profiles of the emission intensity are distinctly different as indicated in Fig. 4.6. It is seen in the figure that the time profile measured during the first shot (curve a) reaches its maximum at much lower pace compared to curve b describing the time history of the primary plasma emission at the 25th shot. It is interesting to note that time profile of the primary plasma emission is similar to curve b appearing at the first shot when the aluminum mask of 1 mm thickness was placed on the sample surface. These observations imply the confinement effect of the crater created by repeated laser irradiations. The formation of primary plasma in the crater allows greater containment of laser energy resulting in a more effective explosive energy source for the creation of shock wave in the surrounding gas.

Fig. 4.7 shows the emission spectra of the primary plasma measured with OMA system in time-integrated mode covering a spectral range between 447 nm and 478 nm using 550 mJ of TEA CO_2 laser pulses on quartz target. Part (a) in this figure is the result of accumulating the spectra of the first 10 shot, namely during the pre-irradiation stage. Part (b) is the result of accumulating spectra of the next 10 shots, namely after the appearance of the secondary plasma, while part (c) is obtained from the following 40 shots. It should be noted that Fig. 4.7 (a) is characterized by continuous emission spectrum without any atomic emission line. The Si I 288.1 nm line was also absent in the UV region of the primary plasma emission. This implies that the Si target is not effectively atomized. It was also observed that the emission area of the primary plasma was a little bit larger than that observed ordinarily, implying less concentrated energy in the plasma. Both of these indications lead to the conclusion that the primary plasma produced is inadequate to generate the strong compression on the surrounding gas required for the generation of the shock wave. In the contrary, several broad atomic lines associated with Si atoms are already visible on top of the continuous emission in Fig. 4.7 (b) and Fig. 4.7 (c) These characteristics closely resemble those of the ordinary primary plasma, as reported previously.[27] Combining these observations with the slow rising emission time profile of the primary plasma in the pre-irradiation stage, as described in Fig. 4.6, we are led to conclude that the plasma observed in the pre-irradiation stage is distinctly different

from that observed previously, and could not serve as the explosion energy source for the generation of shock wave.

One attempted explanation of the influence of the crater is to assume that confinement of the ablated atoms by the crater will result in an effective acceleration of the atoms and thereby enhances the generation of the shock wave. However, this idea must be dismissed simply because this mechanism would lead to faster rise of curve a similar to curve b in Fig. 4.6, which represents the rapid energy accumulation by the ablated atoms. Further, this assumption would lead to the appearance of atomic emission lines in the spectrum. Another possible mechanism considered in this connection is described in the following. As a consequence of the presence of the crater, expansion of fast moving electrons ejected from the target will be suppressed, keeping them relatively close to the target to allow effective absorption of the laser energy via inverse bremsstrahlung process. Note that the absorption coefficient of the laser light due to the inverse bremsstrahlung is proportional to the density of electrons in the initial plasma.[29] As a result, a localized high temperature plasma would be produced leading to strong ablation process which facilitates in turn the shock wave generation. This effective energy accumulation and concentration mechanism is simply missing without the presence of a crater.

Given the crucial role of gas compression and shock wave formation within the framework of our shock wave plasma model, the gas pressure is expected to have important influences on the generation of secondary plasma. It is therefore necessary to investigate the effect of gas pressure in this experiment. The result of measurement on that effect is described in Fig. 4.8. It is seen that increasing the pressure from 2 Torr to 300 Torr results in shorter delay in the occurrence of the secondary plasma. This is in agreement with the expected role of the surrounding gas in the formation of shock wave, and the increased effectiveness of such a role at higher pressure.[27] Nevertheless, the surrounding gas is also known to produce shielding effect at pressure close to 1 atm due to its large absorption of the laser energy. Consequently, the laser energy reaching the sample surface becomes effectively reduced. This explains the opposite effect observed in 1 atm surrounding gas compared to those mentioned above. The associated emission intensity of the induced plasma shows an initial decrease with increasing pressure, but reverses the trend at higher pressure, in good qualitative agreement with our previously reported result.[17,27] It must be pointed out that the intensities detected at 300 Torr and 1 atm are believed to have significant
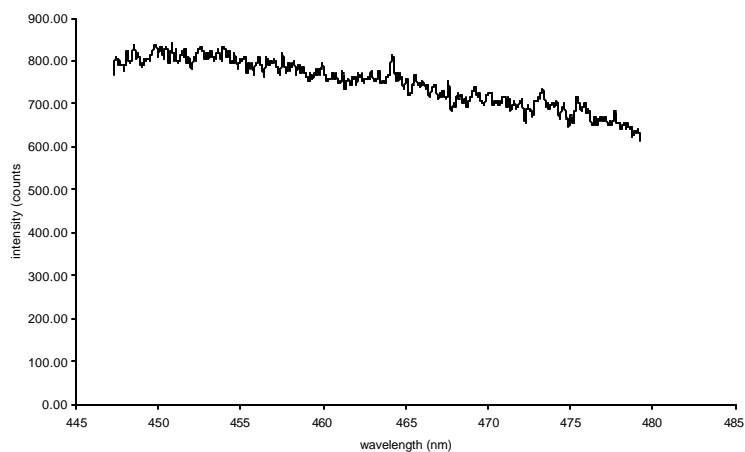
(a)
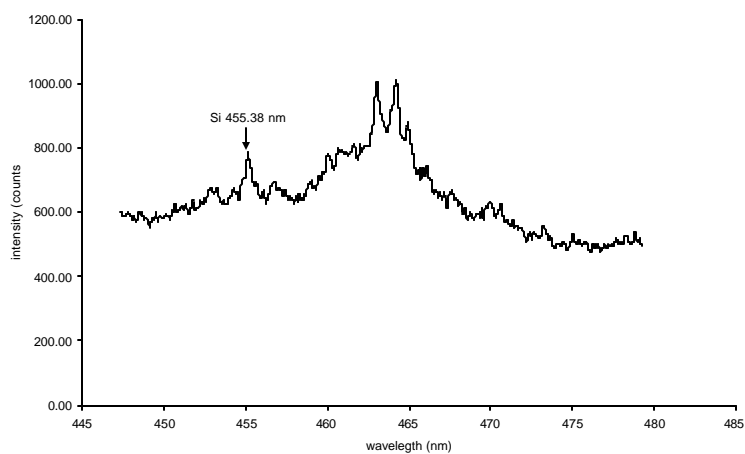
(b)
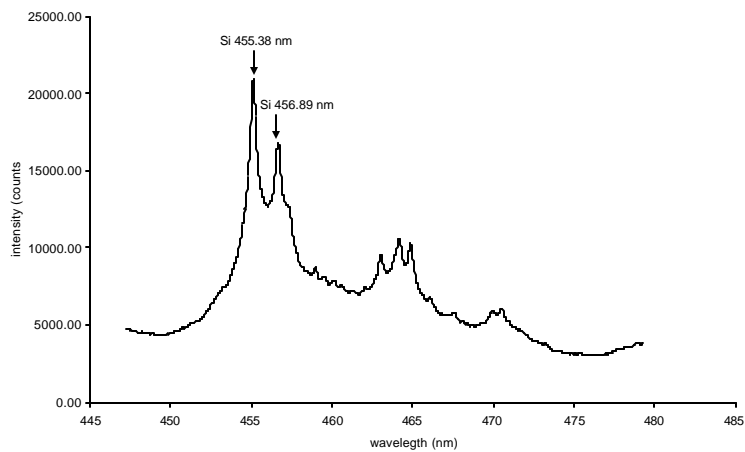
(c)

Fig 4.7. The emission spectra of the primary plasma taken with the use of OMA system using time-integrated mode when 550 mJ pulse of TEA CO$_2$ laser was focused at a fixed point on quartz surface . Part (a) in this figure is the result of accumulating the spectra of the first 10 shot, namely during the pre-irradiation stage. Part (b) is the result of accumulating spectra of the next 10 shots, namely after the appearance of the secondary plasma, while part (c) is obtained from the following 40 shots.

contribution from the primary plasma as the secondary plasma was seen to shrink at those pressure. That is the reason why those intensities tend to decrease slightly after a large number of shots, since the primary plasma generated in the crater becomes more localized inside the hole as the crater deepens with increasing number of shot.

In the same vein, we further examine the issue on the influence of gas density on the generation of the shock wave plasma versus that of the gas pressure itself. In this experiment, different kinds of gas such as helium, nitrogen and argon were employed at properly chosen pressure of 14 Torr, 2 Torr and 1.4 Torr respectively to assure that those surrounding gases are of similar density. The result given in Fig. 4.9 shows that the secondary plasma begins to appear at the 18th shots in helium, at the 21st shots in nitrogen and at the 25th shots in argon. The close proximity in terms of shot number among the pre-irradiation effects in the three cases described above apparently favors the role of the density of the gas as reported previously.[27]
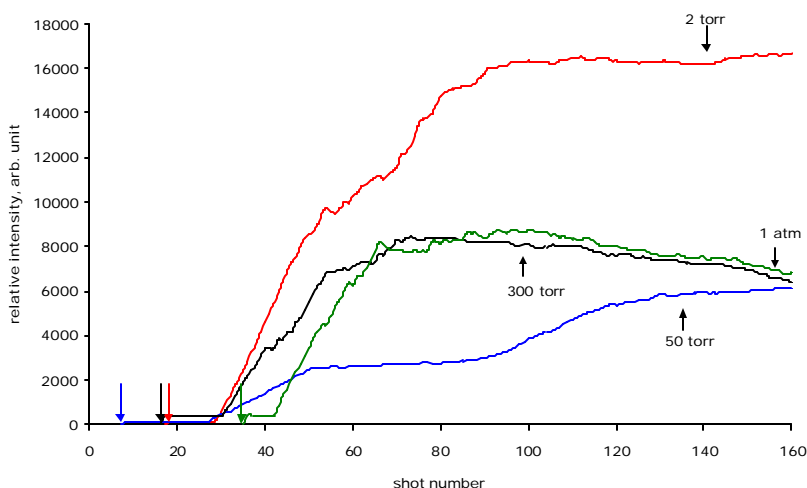
Fig 4.8. The relationship between plasma emission intensity (Si I 288.1 nm) as a function of shot number under different air pressures. The TEA CO$_2$ laser energy was set at 550 mJ and was focused onto quartz sample

It should be stressed here that pre-irradiation effect observed in the experiments with N$_2$ laser (5mJ or so) on quartz sample was also observed when YAG laser (20mJ or so) was focused on glass, quartz, and some stone samples.
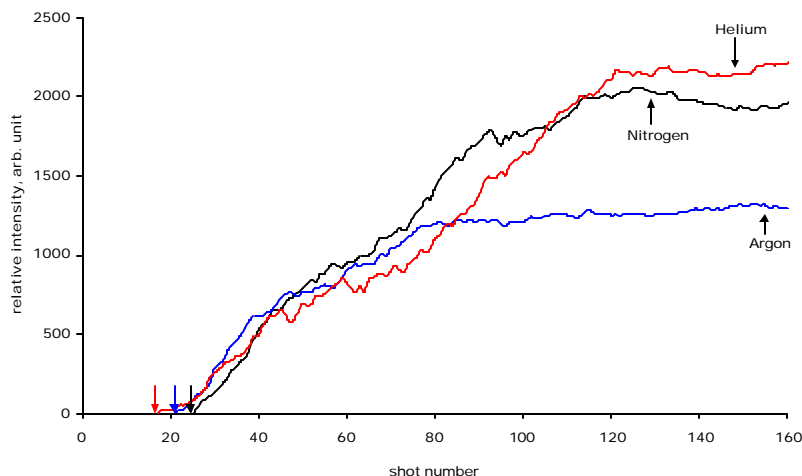
Fig 4.9. The relationship between the secondary plasma emission intensity and laser shot number for different gas kind. The TEA CO$_2$ laser energy was set at 550 mJ and using helium, nitrogen and argon at 14 Torr, 2 Torr and 1.4 Torr, respectively

Once the ordinary normal primary plasma is produced, hydrodynamic confinement of the primary plasma flow will take place in the crater, while the secondary plasma intensity increases. This hydrodynamic confinement effect is indicated by the experimental curve observed after about 45 laser shots presented in Fig. 4.3. It is seen that the primary intensity increases with higher slope together with that of the secondary plasma. The increases of the emission intensity of both the primary and secondary plasma with increasing shot number shown in Fig. 4.4 is also supposed to have the same origin.

As we mentioned before, this pre-irradiation effect did not take place with metal samples. This is probably as a consequence of enhanced preheating of the sample surface, which helped to promote the atomic ablation process. The heating effect was in turn due to the presence of ejected free electrons from the metal during the arrival of the initial part of the laser pulse on the target surface. This free electron cloud at the target surface is known to absorb the laser irradiation effectively by means of inverse bremsstrahlung. In other words, direct heating and softening of target surface by laser irradiation alone is apparently not very effective. Therefore higher laser energy is required to induce strong atomic ablation for the generation of secondary plasma. This explanation is consistent with the fact that the pre-irradiation effect occurring at lower laser energies generally disappears as the energy is raised as we found in quartz and other non metallic samples.

4.1.4. Conclusion

We have shown in this experiment that in contrast to metallic sample, the primary plasma generated at the initial irradiation on a quartz sample does not develop into a secondary plasma as ordinary observed in metallic sample. It is also shown that so called pre-irradiation effect disappears as the crater deepens due to repeated irradiation or upon the application of metal mask of certain thickness on the sample surface. Analysis of the experimental data imply that the elimination of this pre-irradiation effect is supposed to have its origin confinement of the fast electron as well as accumulation and localization of laser absorption takes place by the electron. This results effectively in a localized hot plasma from which atoms are propelled with supersonic speed. Further hydrodynamic confinement also takes place inside the crater after several tens of shots enhancing the shock wave generation process and hence the formation of secondary plasma.

4.2. Confinement Effect of Primary Plasma on Glass Sample Induced by Irradiation of Nd-YAG Laser at Low Pressure

4.2.1 Introduction

In performing micro area analysis using a laser, repeated irradiation onto a fixed position with relatively low pulse energy is required and then a micro crater will be created on the sample surface. Therefore, the effect of the crater on the plasma generation must be thoroughly investigated and understood in order to completely clarify the technique of the laser microprobe emission spectrochemical analysis. Also, the data obtained from this kind of experiment will provide useful knowledge needed in the application of plasma emission for monitoring the laser ablation process itself.

The aim of this experimental work is to report the pre-irradiation phenomenon on the glass samples in relation to the influence of the crater. This will in turn be studied in terms of its confinement effect on the primary plasma generated at a reduced surrounding air pressure. It will be shown that these effects can be understood on the basis of our shock wave model.

4.2.2. Experimental Procedure

The experimental setup is described in Fig 4.10. In this experiment, the 1,064 nm Nd:YAG laser (Spectra Physics, GCR 12S, full power 400 mJ with pulse duration of 8 ns) was operated in manual mode (manually repeating the operation at about 2 Hz) with the output energy being varied from 20 mJ to 48 mJ by using appropriate filters. The laser light was focused with a multilayer lens (f = 100 mm) through a BK-7 window onto the sample surface. The glass sample used in this experiment is museum glass, which contains Si 19%, Ca 4%, Na 9%, Al 0.5% and Mg 0.1%. The sample was placed in a vacuum-tight metal chamber measuring 125 mm X 100 mm X 100 mm. This chamber was evacuated with a vacuum pump and filled with air up to a certain pressure, which was measured and monitored by a digital absolute vacuum meter. Gas flow through the chamber was regulated by a needle valve in the air line and another valve in the pumping line. The sample, together with the entire chamber and the multilayer lens, could be moved in the laser beam direction and a micrometer for movement perpendicular to the laser beam direction. The sample was fixed at the same position during the irradiation.
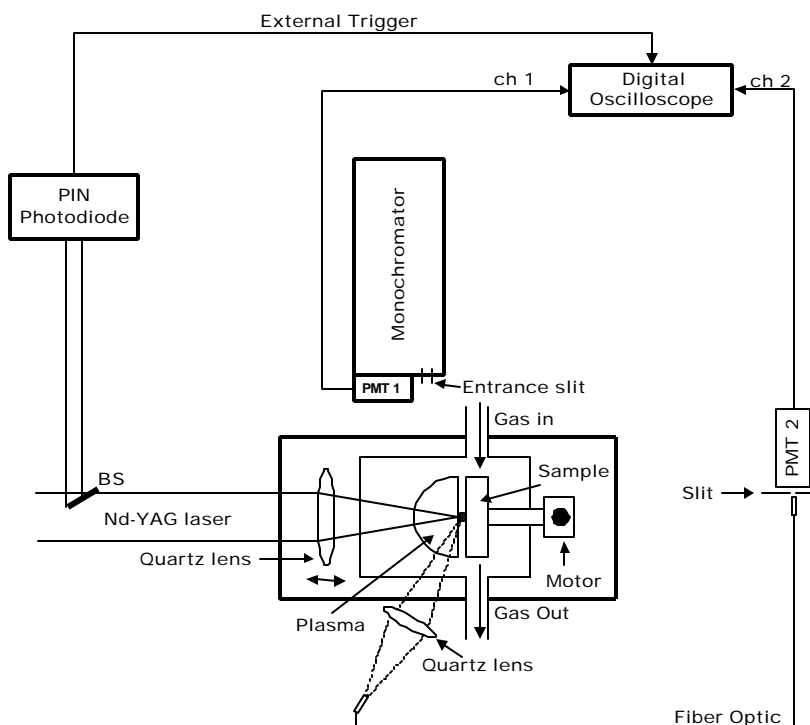
Fig 4.10. Diagram of the experimental setup

For the study of the pre-irradiation effect, a measurement was performed on the spatially integrated emission intensities for both the primary and secondary plasmas. For the secondary plasma measurement, the monochromator (Spex, Czerny Turner configuration, focal length of 750 mm, 1,200 grooves/mm blazed at 500 nm) was set at Si I 288.1 nm, and emission from the secondary plasma was collected directly by the mirror of the monochromator without using an imaging lens. The exit slit of the monochromator was connected to photomultiplier 1 (Hamamatsu IP-28). Meanwhile, for the intensity measurement of the primary plasma, an imaging quartz lens (f = 70 mm) was placed outside the chamber at a position making an angle around 60° with the beam direction. This arrangement allows the primary plasma to be imaged 3:1 onto the entrance of quartz optical fiber so that all of the emission from the image of the primary plasma can be detected. The exit of the fiber was then sent into photomultiplier 2 (Hamamatsu R-1104) after passing through a UV pass filter (UV D36B) and a small aperture which was set in order to allow only the light coming from the image of the primary plasma to come into the photomultiplier. The electric signals from the two photomultipliers were separately fed through a 500 k? resistor to the digital sampling storage scope (HP-54610B).

For the secondary plasma spectrum measurement, the plasma radiation is detected by an optical multichannel analyzer (OMA system, Princeton Instrument IRY-700) attached to a monochromator with a focal length of 150 mm and connected to an optical fiber with its entrance placed in front of the observation window of the vacuum chamber.

In this experiment, the surrounding air was used as a buffer gas and the pressure was kept constant at 2 Torr. The crater sizes produced by the laser bombardment are 160 ?m and 200 ?m in diameter for the pulse energies of the laser light of 20 mJ and 48 mJ, respectively. In addition to this, an investigation was conducted on the confinement effect caused by the presence of a hole in an aluminum mask as well as that caused by the crater created on the sample.

4.2.3. Results and Discussion

When the YAG laser light with around 20 mJ pulse energy was repeatedly focused at a fixed position on the glass sample, a pre-irradiation effect was observed. Namely, at the beginning of the irradiation, only the primary plasma was produced without any secondary plasma appearance, but after several shots, suddenly the secondary plasma was generated.
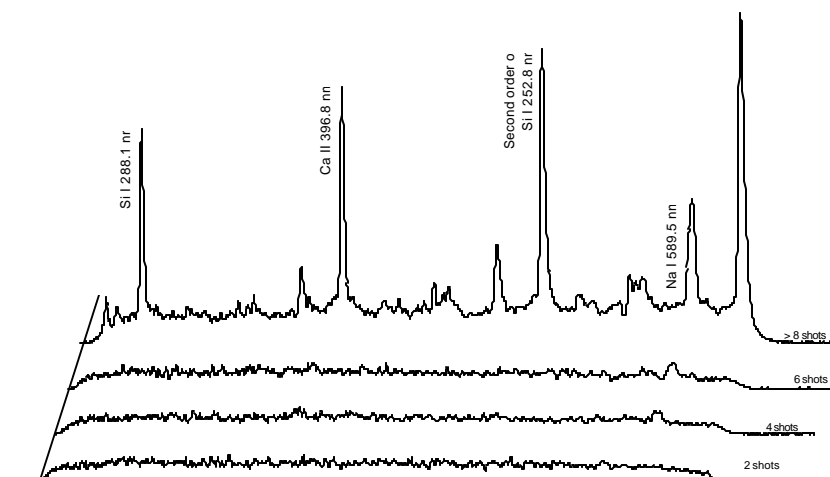
Fig 4.11. Emission spectra taken after several laser shot irradiation at a fixed position of the glass sample; 2 shots, 4 shots, 6 shots and 8 shots. Each spectrum was taken upon single shot irradiation after the pre-irradiation. The laser irradiation was performed using a pulse energy of 28 mJ in the surrounding air pressure of 2 Torr

Figure 4.11 shows the features of the pre-irradiation effect to demonstrate how the emission spectra changes with the number of shots. The spectra were taken at the

pre-irradiation of shot number 2, 4, 6 and 8. The emission spectra were taken using the OMA in time-integrated mode. It is clearly evident that during the initial shots of laser irradiation, with less than six shots only a weak continuous emission spectrum is observed without any atomic emission lines. This means that the secondary plasma is not produced until the sixth shot. On the other hand, the emission spectrum taken at nine shots contains several atomic emission lines together with the enhanced continuous emission spectrum.

A similar pre-irradiation effect was observed in other samples, such as quartz and some kinds of stone of which the host element is silicon. However, phenomenon such as the pre-irradiation effect have never been observed on metal samples in any range of the pulse energy of laser light.
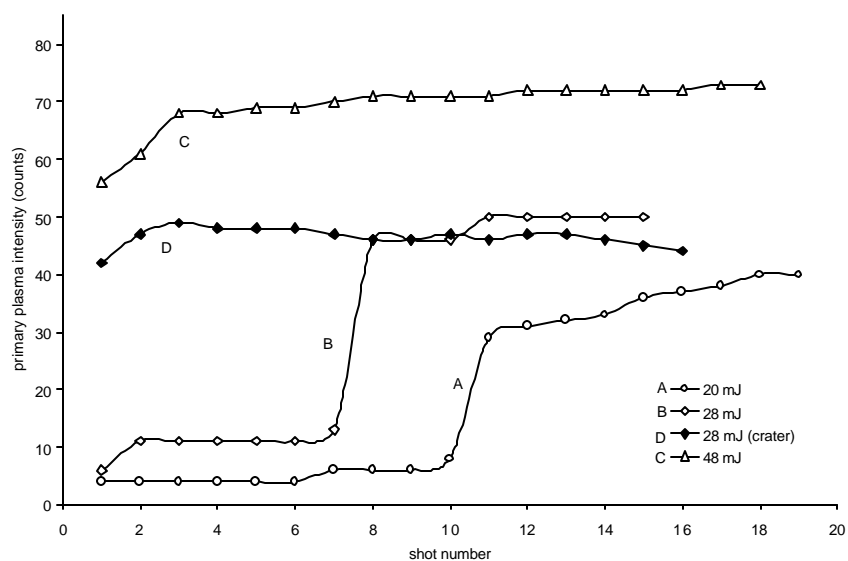
Fig 4.12. Relationship between the time-integrated emission intensity of the primary plasma and the laser shot number at different laser energies, A for 20 mJ, B for 28 mJ, C for 48 mJ and D. Curve D was obtained in the experiment where the pre-irradiation was caused with 10 shots using 48 mJ pulse energy and after sufficient cooling time the irradiation was resumed at the same position with the same pulse energy of 28 mJ in the surrounding air pressure of 2 Torr

Figure 4.12 shows how the intensity of the primary plasma changes with the shot number for different pulse energies of the YAG laser. The intensity of the primary plasma was detected in time-integrated mode. In Fig 4.12, it is evident that when the pulse energy of the laser light is relatively low, the primary plasma is weak in its intensity at the beginning of the subsequent irradiation; however, discrete increments of the primary plasma emission take place at 11 shots for 20 mJ pulse energy and at eight shots for 28 mJ, and after the increment, the emission increases slowly or

remains almost constant. In contrast to this, for 48 mJ pulse energy, from the first shot the emission intensity reaches a high value and no pre-irradiation effect is observed. The temporal behavior of the primary plasma was also detected by using a 500 ? load resistance attached to the photomultiplier. The primary plasma signal started with a growth time about 50 ns decayed with a time constant of around 200 ns.
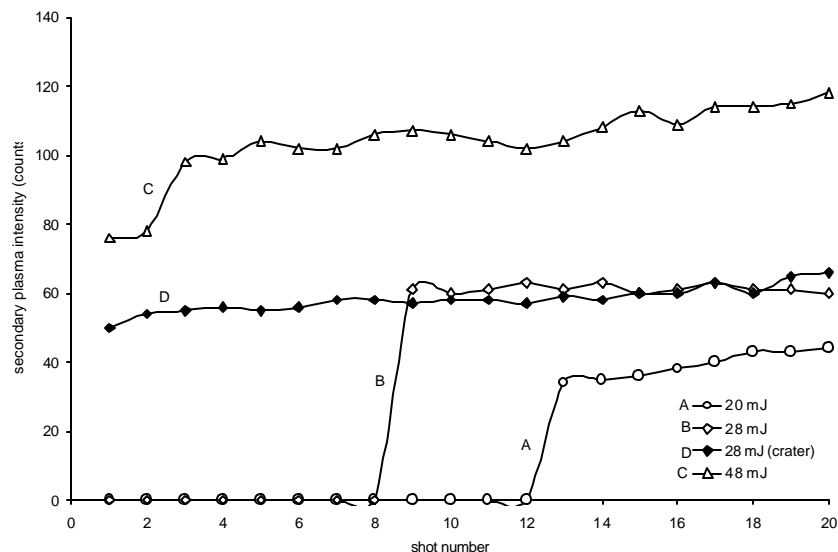
Fig 4.13. Relationship between the total emission intensity of the secondary plasma (Si I 288.1 nm) and the laser shot number at different laser energies. These data were obtained simultaneously with those in Fig 4.12, and notations A, B, C and D have the same meaning as in Fig 4.12. The data taken in surrounding air pressure at 2 Torr

Figure 4.13 shows how the spatially and time-integrated emission of the secondary plasma changes with the shot number for different pulse energies of the YAG laser. The data in Figs 4.12 and 4.13 were taken simultaneously using the experimental setup shown in Fig 4.10. The features of the curves in Fig 4.13 are similar to those shown in Fig 4.12. However, it should be noted that for the secondary plasma, no emission takes place before the sudden increment. Also, the sudden increment occurred with a one or two-shot delay compared to the case for the primary plasma; namely, for 20 mJ pulse energy, the increment occurs at 13 shots and for 28 mJ it occurs at nine shots. The temporal behavior of the secondary plasma signal was also detected by using the 500 ? load resistance. The growth time of the signal was about 500 ns and the decay time was about 2 ? s.

In order to clarify the reason for the pre-irradiation effect, three possible mechanism were considered; a preheating effect due to the repeated irradiation, a

confinement effect due to the crater created during the repeated irradiation, and the effect of optical change in the glass sample, which might increase the absorption coefficiency against the laser light. The last possibility can be eliminated because the wavelength of the laser used in this experiment is infrared, 1.06 ?m, and the photon energy is too low to induce such photochemical reaction in the sample under this kind of pulse energy. Also, during the pre-irradiation, vaporization takes place from the sample surface during every shot. Therefore, under the repeated irradiation the accumulation of such a photochemical could not occur.

In order to clarify whether the preheating effect is the major cause of the pre-irradiation effect, the following experiment was carried out. The laser radiation was repeated with a very low repetition rate at the same energy. It was confirmed that even in such a case almost identical curves were obtained for the relationship between the emission intensities and the shot numbers. This implies that the thermal process is not responsible for the pre-irradiation effect.

In order to confirm that the pre-irradiation effect is related to the confinement effect, due to the crater, another experiment was carried out. The laser irradiation was set at an energy of 48 mJ and irradiation was repeated up to ten shots, and then stopped to confirm the clear presence of the crater with a depth of about 3 mm. Then, the laser irradiation was resumed at the same position with a lower pulse energy of 28 mJ. In this case, no pre-irradiation effect was observed, which is different from the curves B in Fig 4.10 and 4.11. In other words, both the primary and the secondary plasma were produced from the first shot, as shown by the curves D in Figs 4.12 and 4.13. This indicates that if the primary plasma is produced in the deep crater, the threshold laser energy can be considerably reduced by the confinement effect due to the crater. This confinement effect due to crater was confirmed by another experiment. A mask made of an aluminum plate (1 mm thickness), which had a hole with a diameter of 1 mm, was firmly attached to the surface of the glass, and laser irradiation of 28 mJ was made through the hole of the mask onto the new glass surface. It was found that both primary and secondary plasma could be generated at the first shot. Therefore, we can conclude that the pre-irradiation effect is due to the confinement taking place in the hole or crater. In order to clarify the physical implications of this confinement, two possible mechanisms were considered: 1) confinement of the initial fast electron expansion, and 2) confinement of the primary

plasma to achieve geometrical focusing of the plasma flow. The key point to be considered is why the primary plasma emission intensity is enhanced by the confinement. If the laser pulse energy were fully absorbed by the interaction with the material, the time-integrated emission intensity of the primary plasma would be almost the same irrespective of the presence of the confinement, even though the time behavior of the emission signal would change depending on whether the primary plasma induces an explosion in the moment or not. However, as shown by curves A and B in Fig 4.12, the time-integrated emission intensity of the primary plasma is weak in the pre-irradiation stage. This implies that in this stage only a limited part of the laser light is absorbed. In fact, the glass sample is basically transparent at the wavelength of the laser light. We assume that the enhancement of the emission of the primary plasma by the crater is due to the increment of the absorption of the laser light. Namely, it is believed that because of the presence of the crater or hole the laser light is more efficiently absorbed in the initial plasma via inverse bremsstrahlung due to the suppression of the expansion of the fast electrons ejected from the target;[28] the absorption coefficient of the laser light due to the inverse bremsstrahlung is proportional to the density of electrons in the initial plasma.[29] Once the intense primary plasma is produced by sufficient absorption, confinement of the hydrodynamics of the primary plasma motion will take place due to the geometrical focusing of plasma flow in the crater, and as result the secondary plasma is produced.

In our previous study, we have proposed the shock wave model to explain the generation of the secondary plasma as follows.[9] First, the primary plasma is produced by the bombardment of the laser light. From the primary plasma, atoms gush out at high speed. The movement of the gushed atom is interrupted by collision with the surrounding gas molecules, and stagnation takes place at a certain distance from the primary plasma. By adiabatic compression, high-temperature plasma is produced. The most important point of the shock wave model is that the energy for producing the secondary plasma is supplied in the form of kinetic energy, by which atoms are excited. Clearly, if the speed of the gushing atoms has less energy, insufficient compression takes place, and the secondary plasma will not be produced. This insufficient compression case corresponds to the data plots before the sudden increment in curves A and B in Fig 4.13, where no emission is observed. Once the crater depth attains a certain value through repeated irradiation, the confinement effect due to the wall of the crater takes place and enhances the generation of the intense

primary plasma, according to the process described above. Under this condition, if a strong explosion from the primary plasma takes place and thus, favorable conditions are provided for forming the secondary plasma, and atoms can gush out from the primary plasma with sufficiently high speed to form the shock wave. This is how the primary plasma grows and subsequently the secondary plasma starts to be generated. It should be noted here that the pre-irradiation effect reported in this paper can be interpreted well according to our shock wave model, while it basically cannot be explained satisfactorily by other models such as the electron-ion recombination process[30,31] or electron collision process,[32] even though such processes may occur to some extent during the laser ablation.

As shown in Figs 4.12 and 4.13, the pre-irradiation effect does not occur when we use a pulse energy higher than 48 mJ. Therefore, if we use a relatively high-power pulse energy to generate plasma, the pre-irradiation effect can be completely eliminated. However, we must select conditions favorable for practical spectrochemical analysis. As we reported with reducing the laser pulse energy, the ion production rate decreases; as a result, the background reduces and sensitivity increases. Therefore, we must employ a laser with a relatively low pulse energy in the laser-induced shock wave spectroscopy. In such case, the pre-irradiation effect cannot be neglected when we perform analysis on glass or rock samples.

4.2.4. Conclusion

We have shown in this study that in contrast to metallic samples, a characteristic pre-irradiation effect is observed on a glass sample when the pulse energy is relatively low. During the pre-irradiation period, only the primary plasma is observed with increasing intensity. The generation of secondary plasma takes place only after the first few laser shots. It is demonstrated in this experiment that the pre-irradiation effect has its origin in the failure of shock wave formation in the initial laser irradiation. The occurrence of shock wave and secondary plasma in the shots is shown to be connected with the creation of a crater on sample surface due to repeated bombardment on the sample. This gives rise to the much needed confinement effect for the formation of shock wave and secondary plasma. In addition to explaining the pre-irradiation effect further confining the shock wave plasma model, this experiment result also provide the basis for extending the LISPS application to soft sample.

Chapter Five

GENERAL CONCLUSION

It is shown that laser induced shock wave plasma spectroscopy method which has proved highly favorable for spectrochemical analysis of metallic samples, can not be applied directly to non metallic soft samples. This is explained as a consequence of the failure in the generation of secondary plasma due to the weakened expulsion of atoms by the soft surface which tends to absorbs the recoil energy in the form of surface deformation. Therefore, atoms gushing out from the primary plasma do not acquire sufficient speed to form a shock wave. It is demonstrated nevertheless that the presence of sub target behind the soft sample helps to overcome this weakness and allows the generation of secondary plasma adequate for spectrochemical analysis. The experimental results obtained in this study, for both low and high pressure surrounding gases, also offer additional evidence in support of the shock wave model which explains the mechanism of laser-induced shock wave plasma.

Another interesting and important feature revealed in this study is a characteristic pre-irradiation effect observed in the case of non metallic hard target when a low power pulsed laser is used. During this pre-irradiation period, the primary plasma generated at the initial stage does not develop into a secondary plasma as ordinarily observed in the metallic case. It is also found that the pre-irradiation effect disappears as the crater deepens due to repeated initial irradiations. Analysis of the experimental data clearly indicates that the pre-irradiation effect is characterized by the absence of shock wave in the surrounding gas. On the contrary, a shock wave is detected in conjunction with the appearance of secondary plasma after a certain number of repeated shots on the same spot. It is suggested in this connection that plasma confinement effect plays the main role in the effective enhancement of the shock wave generation and hence the appearance of secondary plasma.

In a further experiment employing a mask/artificial crater of appropriate thickness on the surface of non metallic hard sample, the pre-irradiation effect was completely eliminated. In addition to confirming the role of plasma confinement in overcoming the pre-irradiation effect, the experimental result also introduces a useful

means to avoid the undesirable damage on the sample surface for laser microprobe analysis.

In short, we have successfully demonstrated in this study, useful secondary plasma can be simply generated by applying a sub target behind the non metallic soft sample and placing a small metallic mask on the surface of non metallic hard sample. As a result, the LISPS method can be readily extended for highly sensitive and rapid quantitative analysis to non metallic samples.

REFERENCES

1. J.D. Ingle, Jr. and S.R. Crouch: *Spectrochemical Analysis*, eds. J.D. Ingle, Jr. and S.R. Crouch (Prentice-Hall, Inc., New Jersey, 1988)

2. L.J. Radziemski and D.A. Cremers: *Laser induced Plasma and Applications*, eds. L.J. Radziemski and D.A. Cremers (Marcel Dekker, New York, 1989)

3. J. Hecht: *The Laser Guide Book*, eds. J. Hecht (McGraw-Hill, Singapore, 1986)

4. F. Brech and L. Cross: *Optical Microemission Stimulated by a Ruby Laser*, Appl. Spectrosc. **16** (1962) 59

5. K. Kagawa, M. Ohtani, S. Yokoi and S. Nakajima: *Characteristics of the Plasma Induced by the Bombardment of N_2 Laser Pulse at Low Pressures*; Spectrochim. Acta, **39B** (1984) 525

6. K. Kagawa, K. Kawai, M. Tani and T. Kobayashi: *XeCl Excimer Laser-Induced Shock Wave Plasma and Its Application to Emission Spectrochemical Analysis*; Appl. Spectrosc. **48** (1994) 198

7. H. Kurniawan, M.O. Tjia, M. Barmawi, S. Yokoi, Y. Kimura and K. Kagawa: *A Time- Resolved Spectroscopic Studies on the Shock Wave Plasma Induced by the Bombardment of A TEA CO_2 Laser*; J. Phys. D: Appl. Phys., **28** (1995) 879

8. H. Kurniawan, S. Nakajima, J. E. Batubara, M. Marpaung, M. Okamoto and K. Kagawa: *Laser-Induced Shock Wave Plasma in Glass and Its Application to Elemental Analysis*; Appl. Spectrosc., **49** (1995) 1067

9. H. Kurniawan, Y. Ishikawa, S. Nakajima and K. Kagawa: *Characteristics of the Secondary Plasma Induced by Focusing A 10 mJ XeCl Excimer Laser at Low Pressures*; Appl. Spectrosc., **51** (1997) 1769

10. K. Kagawa and S. Yokoi: *Application of the N_2 Laser Microprobe Spectrochemical Analysis*; Spectrochim. Acta, **B37** (1982) 789

11. M. Tani, H. Kurniawan, H. Ueda, K. Mizukami, K. Kawai and K. Kagawa: *Reflection and Diffraction of Laser Plasma Induced by Bombardment of TEA CO_2 Laser at Low Pressures*; Jpn. J. Appl. Phys., **32**, 9A (1993) 3838

12. W.S. Budi, H. Suyanto, H. Kurniawan, M. O. Tjia and K. Kagawa: *Shock Excitation and Cooling Stage in the Laser Plasma Induced by Q-Switch Nd-YAG Laser at Low Pressure*s; Appl. Spectrosc., **53** (1999) 719

13. M. Marpaung, M. Pardede, R. Hedwig, H. Kurniawan, T.J. Lie and K. Kagawa: *Coincidence of Density Jump and Plasma Emission Front Induced by TEA CO$_2$ Laser Bombardment at Low and High Pressures*; Jpn. J. Appl. Phys., **39**, 6B (2000) 601

14. R.E. Russo: *Laser Ablation*; Appl. Spectrosc., **49**, 9 (1995) 14A

15. N. Omenetto: *Role of Lasers in Analytical Atomic Spectroscopy: Where, When and Why – Plenary Lecture*; J. Anal. Atomic Spectrom., **13** (1998) 385

16. J.W. Robinson: *Atomic Spectroscopy*, eds. J.W. Robinson (Marcel Dekker, New York, 1996)

17. K. Kagawa and H. Kurniawan: *Laser-Induced Shock Wave Plasma Spectroscopy*; Trends in Appl. Spectrosc., **2** (1998) 1

18. D.A. Cremers and L.J. Radziemski: *Laser Spectroscopy and Its Application*, eds. L.J. Radziemski, R.W. Solarz and J.A. Paisner (Marcel Dekker, New York, 1987)

19. T. Karlinski and G. Johnson: *Developments in Atomic Plasma Spectrochemical Analysis*, eds. R.M. Barnes (Heyden and San Ltd., 1981)

20. M.M. Suliyanti, R. Hedwig, H. Kurniawan and K. Kagawa: *The Role of Sub-Target in the TEA CO$_2$ Laser-Induced Shock-Wave Plasma*; Jpn. J. Appl. Phys., **37**, 12A (1998) 6628

21. L.I. Sedov: *Similarity and Dimensional Method in Mechanics* (Academic Press, New York and London, 1959)

22. M. Tani, K. Mizukami, H. Ueda, Y. Dehuchi, Y. Takagi and K. Kagawa: *Emission Spectrochemical Analysis of Fluorine in Biological Samples With a Shock Wave Plasma Induced by TEA CO$_2$ Laser*, J. Spectrosc. Soc. Jpn., **41** (1992) 265

23. J.H. Yoo, S.H. Jeong, R. Greif and R.E. Russo: *Explosive Change in Crater Properties During High Power Nanosecond Laser Ablation of Silicon*; J. Appl. Phys., **88**, 3 (2000) 1638

24. O.V. Barisov, X.L. Mao and R.E. Russo: *Effects of Crater Development on Fractionation and Signal Intensity During Laser Ablation Inductively Coupled Plasma Mass Spectrometry*; Spectrochim. Acta, **B55** (2000) 1693

25. H. Kurniawan, T.J. Lie, N. Idris, M.O. Tjia, M. Ueda and K. Kagawa: *Detection of the Density Jump in the Laser-Induced Shock Wave Plasma Using Low energy Nd:YAG Laser at Low Pressures of Air*; J. Spectrosc. Soc. Jpn., **50**, 1 (2001) 13

26. H. Kurniawan, K. Lahna, T.J. Lie, K. Kagawa and M.O. Tjia: *Detection of Density Jump in Laser-Induced Shock Wave Plasma Using a Rainbow Refractometer*; Appl. Spectrosc., **55**, 1 (2001) 92

27. A.M. Marpaung. H. Kurniawan, M.O. Tjia and K. Kagawa: *Comprehensive Study on the Pressure Dependence of Shock Wave Plasma Generation Under TEA CO_2 Laser Bombardment on Metal Sample*; J. Phys. D: Appl. Phys., **34** (2001) 758

28. X.L. Mao, W.T. Chan, M.A. Shannon and R.E. Russo: *Plasma Shielding During Picosecond Laser Sampling of Solid Materials by Ablation in He versus Ar Atmosphere*; J. Appl. Phys., **74** (1993) 4915

29. A.F. Gibson, T.P. Hughes and C.L.M. Ireland: *CO_2 Laser Generation of Plasma for Spectroscopy and Spectrochemical Analysis*; J. Phys. D **4** (1971) 1527

30. W. T. Silvast, L. H. Szeto and O. R. Wood II: *Recombination Lasers in Expanding CO_2 Laser-Produced Plasmas of Argon, Krypton and Xenon*; Appl. Phys. Lett., **31** (1977) p. 334

31. J.M. Green, W.T. Silfvast and O.R. Wood: *Evolution of A CO_2-Laser-Produced Cadmium Plasma*; J. Appl. Phys., **48** (1977) 2753

32. D. B. Geohegan: *Diagnostics and Characteristics of Pulsed Laser Deposition Laser Plasmas, in Pulsed Laser Deposition of Thin Films*; (D. B. Chrisey and G. K. Hubler, Eds, John Wiley & Sons, New York, 1994)

33. C.W. Ng, W.F. Ho, and N.H. Cheung: *Spectrochemical Analysis of Liquids Using Laser-Induced Plasma Emission: Effects of Laser Wavelength on Plasma Properties*; Appl. Spectrosc., **51**, 7 (1997) 976

34. J.H. Yoo, S.H. Jeong, R. Greif, and R.E. Russo: *Explosive Change in Crater Properties During High Power Nanosecond Laser Ablation of Silicon*; J. Appl. Phys., **88**, 3 (2000) 1638

35. K. Kagawa, Y. Matsuda, S. Yokoi and S. Nakajima: *Nitrogen Laser Ablation Analysis Using the Primary Plasmas a Standard for the Qualification of Vaporized Atoms*; J. Anal. At. Spectrom., **3** (1998) 415

LIST OF SCIENTIFIC PUBLICATIONS

International Publications

1. M.M. Suliyanti, <u>R. Hedwig</u>, H. Kurniawan, and K. Kagawa: *The Role of a sub-target in the TEA CO$_2$ Laser-Induced Shock Wave Plasma*, Jpn. J. Appl. Phys. **37**, 12 (1998) pp. 6628-6632

2. K. Kagawa, T.J. Lie, <u>R. Hedwig</u>, S. Nur Abdulmajid, M.M. Suliyanti, and H. Kurniawan: *Sub Target Effect on Laser Plasma Generated by Transversely Excited Atmospheric CO$_2$ Laser at Atmospheric Gas Pressures*, Jpn. J. Appl. Phys., **39**, 1, 5A (2000) pp. 2643-2646

3. A.M. Marpaung, M. Pardede, <u>R. Hedwig</u>, H. Kurniawan, and K. Kagawa: *Coincidence of Density Jump and the Front of Plasma Emission Induced by TEA CO$_2$ Laser Bombardment at Low and High Pressures*, Jpn. J. Appl. Phys., **39**, 6B (2000) pp. L601-L603

4. A.M. Marpaung, <u>R. Hedwig</u>, M. Pardede, H. Kurniawan, M.O. Tjia, and K. Kagawa: *Shock Wave Plasma Induced by TEA CO$_2$ Bombardment on Glass Samples at High Pressures*, Spectrochim. Acta Part B; At. Spectrom. **B55**, 10 (2000) pp. 1591-1599

5. <u>R. Hedwig</u>, H. Kurniawan, and K. Kagawa: *Confinement Effect of Primary Plasma on Glass Sample Induced by Irradiation of Nd-YAG Laser at Low Pressures*, Jpn. J. Appl. Phys. **40** 10 (2001) pp. 5938-5941

6. <u>R. Hedwig</u>, M.O. Tjia, K. Kagawa, and H. Kurniawan: *Confinement Effect in Enhancing Shock Wave Plasma Generation at Low Pressure by TEA CO$_2$ Laser Bombardment on Quartz Sample*, Spectrochim. Acta Part B (in submission)

International Conferences

1. W.S. Budi, <u>Rinda</u>, M. Pardede, H. Kurniawan, and K. Kagawa: *Effect of Focusing of Laser Irradiation on Spectral Emission of Laser-Induced Shock-wave Plasma at Reduced Air Pressure,* Association of Asia Pacific Physics Conference, Yogyakarta, Indonesia (1998)

2. R. Hedwig, H. Kurniawan, M.M. Suliyanti, S. Nur, and K. Kagawa: *The Role of Sub-target for Soft Sample in Laser-Induced Shock Wave Plasma*, International

Laser Sensing Symposium and 20th Japanese Laser Sensing Symposium, Fukui, Japan (1999), proceeding pp. 81-84

3. M.M. Suliyanti, R. Hedwig, and H. Kurniawan: *Emission Spectrochemical Analysis of Gold Alloy Using Primary Plasma Standardization*, International Conference on Electrical, Electronics, Communication and Information, CECI 2001, March 7-8, Jakarta, Indonesia, Proc., pp. OL1-OL5

National Publication

1. Rinda, S.P. Liawatimena, dan S. Lukas: *Plotter Berbasis Mikrokontroler*, Jurnal Teknik Komputer, **1**, 1 (1995)

2. W.S. Budi, M. Pardede, H. Kurniawan, Rinda, and K. Kagawa: *Effect of Focusing of Laser Irradiation on Spectral Emission of Laser Induced Shock Wave Plasma at Reduced Air Pressure*, Physics Journal – Indonesia Physical Society, **2**, 1 (1999) pp. 84-91

3. R. Hedwig, T.J. Lie, and H. Kurniawan: *Comparison of Confinement Effect in Enhancing Shock Wave Plasma Generation at Low Pressure between TEA CO$_2$ and Nd-YAG Lasers on Quartz Sample*, Physics Journal – Indonesia Physical Society, **A5**, 0203 (2002) pp. 1-6

National Conference

1. W.S. Budi, W.T. Baskoro, and Rinda: *Pengaruh Ketepatan Pemfokusan pada Ukuran Crater dan Massa Terevaporasi Akibat Iradiasi Laser Nd-YAG*, Prociding Seminar Nasional Fisika Terapan dan Lingkungan, 1997

2. M.M. Suliyanti dan Rinda: *Peranan Sub Target Dalam Pembangkitan Gelombang Kejut Plasma pada Target Lunak*, Prociding Seminar Nasional Fisika Terapan dan Lingkungan, 1997

3. H. Kurniawan, R. Hedwig, K. Kagawa, and M.O. Tjia: *Characteristics of Laser-Induced Shock Wave Plasma generated at 0.5 Torr*, XVIII National Physics Conference, Serpong, Indonesia, 2000

4. H. Kurniawan, T.J. Lie, R. Hedwig, and K. Kagawa: *A Short Summary of Time-Resolved Spectroscopic Study in the Laser Plasma Generated by Irradiation of High Power Short Pulse Laser on Metal Samples Under Reduced Gas Pressure*, ICOLA 2002 Symposium (in submission)

CURRICULUM VITAE

Author Name   : Rinda HEDWIG

Date and Place of Birth : June, 20th 1973 in Surabaya

Gender   : Female

Home Address   : Tomang Tinggi IV No. 10,

                                      Gg. Buntu RT 04/06, Jakarta 11440

Phone   : +62 21 5681885 / +62 818 195976

Email Address   : arindaho@yahoo.com

Personal Homepage   : http://www.geocities.com/marinda7899

Office Address   : Bina Nusantara University,

                                      Hardware Laboratory,

                                      KH. Syahdan 9, Jakarta 11480

Office Phone/Fax   : +62 21 5345830 / +62 21 5300244

Professional Homepages   : http://www.geocities.com/spectrochemical

                                      http://www.binus.ac.id

                                      http://www.geocities.com/pkm_binus

                                      http://www.geocities.com/klpkm

Education:

- Computer Science degree in Computer Engineering, STMIK Bina Nusantara, Jakarta, year 1995
- Master of Science degree in Opto-Electrotechniques and Laser Applications, Graduate Program in Opto-Electrotechniques and Laser Applications, University of Indonesia, Jakarta, year 1998